Tellus (2001), 53B, 615–645
Printed in UK. All rights reserved

TELLUS
ISSN 0280–6509

A comparison of large-scale atmospheric sulphate aerosol models (COSAM): overview and highlights

By L. A. BARRIE[1,*], Y. YI[2], W. R. LEAITCH[3], U. LOHMANN[4], P. KASIBHATLA[5], G.-J. ROELOFS[6], J. WILSON[7], F. McGOVERN[8], C. BENKOVITZ[9], M. A. MÉLIÈRES[10], K. LAW[11], J. PROSPERO[12], M. KRITZ[13], D. BERGMANN[14], C. BRIDGEMAN[11], M. CHIN[15], J. CHRISTENSEN[16], R. EASTER[1], J. FEICHTER[17], C. LAND[17], A. JEUKEN[18], E. KJELLSTRÖM[19], D. KOCH[20] and P. RASCH[21], [1]*Fundamental Science Division, Pacific Northwest National Laboratory, PO Box 999, Richland, WA 99352, USA;* [2]*East Giant Science and Technology Inc., 45 Rock Fernway, Toronto, ON, M2J 4N3, Canada;* [3]*Climate and Atmospheric Science Directorate of Environment Canada, 4905 Dufferin St., Toronto, ON, M3H 5T4, Canada;* [4]*Atmospheric Science Program, Physics Department, Dalhousie University, Halifax, NS, Canada;* [5]*Nicholas School of the Environment, Duke University, Durham, NC, USA;* [6]*(IMAU) Utrecht University, Utrecht, The Netherlands;* [7]*European Commission Environment Institute, Ispra, Italy;* [8]*Department Experimental Physics, University College, Dublin, Ireland;* [9]*Environmental Science Department, Brookhaven National Laboratory, Upton, NY, USA;* [10]*Laboratoire de Glaciologie et Geophysique de l'Environnement, Grenoble, France;* [11]*Centre for Atmospheric Science, Department of Chemistry, University of Cambridge, UK;* [12]*University of Miami, Miami, FL, USA;* [13]*Atmospheric Sciences Research Center, State University of New York, Albany, NY, USA;* [14]*Atmospheric Science Division, Lawrence Livermore National Laboratory, Livermore, CA, USA;* [15]*NASA Goddard Space Flight Center, Greenbelt, MD, USA;* [16]*National Environmental Research Institute, Roskilde, Denmark;* [17]*Max Planck Institute for Meteorology, Hamburg, Germany;* [18]*Royal Netherlands Meteorological Institute (KNMI), De Bilt, The Netherlands;* [19]*Department of Meteorology, Stockholm University, S-106 91 Stockholm, Sweden;* [20]*Goddard Institute for Space Studies, Department of Geology and Geophysics, New Haven, CT, USA;* [21]*National Center for Atmospheric Research (NCAR), Boulder, CO, USA*

(Manuscript received 23 February 2000; in final form 2 April 2001)

ABSTRACT

The comparison of large-scale sulphate aerosol models study (COSAM) compared the performance of atmospheric models with each other and observations. It involved: (i) design of a standard model experiment for the world wide web, (ii) 10 model simulations of the cycles of sulphur and $^{222}Rn/^{210}Pb$ conforming to the experimental design, (iii) assemblage of the best available observations of atmospheric $SO_4^=$, SO_2 and MSA and (iv) a workshop in Halifax, Canada to analyze model performance and future model development needs. The analysis presented in this paper and two companion papers by Roelofs, and Lohmann and co-workers examines the variance between models and observations, discusses the sources of that variance and suggests ways to improve models. Variations between models in the export of SO_x from Europe or North America are not sufficient to explain an order of magnitude variation in spatial distributions of SO_x downwind in the northern hemisphere. On average, models predicted surface level seasonal mean $SO_4^=$ aerosol mixing ratios better (most within 20%) than SO_2 mixing ratios (over-prediction by factors of 2 or more). Results suggest that vertical mixing

* Corresponding author.
email: leonard.barrie@pnl.gov

Research by BNL investigators was performed under the auspices of the U.S. Department of Energy under Contract No. DE-AC02-98CH10886.

from the planetary boundary layer into the free troposphere in source regions is a major source of uncertainty in predicting the global distribution of $SO_4^=$ aerosols in climate models today. For improvement, it is essential that globally coordinated research efforts continue to address emissions of all atmospheric species that affect the distribution and optical properties of ambient aerosols in models and that a global network of observations be established that will ultimately produce a world aerosol chemistry climatology.

1. Introduction

Atmospheric aerosols play a key rôle in many important environmental issues including climate change, stratospheric ozone depletion, oxidant/smog, acid rain and toxic chemicals. Internationally coordinated science assessments of the state of knowledge of these issues are routinely conducted (e.g., the IPCC Assessments of Climate Change, the International Ozone Assessment, numerous regional assessments in major source regions). Large-scale models for the troposphere/stratosphere system that simulate for aerosols and their gaseous precursors, the processes of emissions, transport/dispersion, chemical/physical transformation and removal play a central rôle in these assessments. These models abound and their results appear frequently in scientific literature. There is a need to define their performance relative to each other and to current knowledge of aerosol occurrence and processes.

This paper and two companion papers (Lohmann et al., 2001; Roelofs et al., 2001) describe the experimental design and results of an internationally coordinated study that focussed on a COmparison of large-scale Sulphate Aerosol Models (COSAM). When COSAM was initiated in February 1998, sulphates were the only major aerosol types (e.g., sulphates, black carbon, organic carbon, sea salt, soil dust and nitrates) for which there were a sufficient number of global models and sufficient knowledge of occurrence and processes on a global domain to warrant an international comparison. COSAM is one of a series of model comparisons that has been sponsored over the years by the World Climate Research Program. In 1990, 13 models simulating the atmospheric distribution of CFC-11 were compared (Pyle and Prather, 1996). In 1993, a second comparison of sub-grid scale tracer transport was conducted with 22 models simulating the atmospheric cycle of ^{222}Rn (Jacob et al., 1997). In 1995, the ability of 15 models to simulate the transport and scavenging of sulphur and ^{222}Rn was compared (Rasch et al., 2000b).

The results of the last comparison study (Rasch et al., 2000b) were particularly relevant to COSAM. One conclusion was that "models differ dramatically in their simulations of soluble species and observations (particularly at altitude) do not yet provide us with strong constraints on the reality of simulations". Thus, an emphasis in the experimental design of COSAM was on the use of more observations including those in the vertical. A second conclusion was that "transport of SO_x (i.e., $SO_4^=$ plus SO_2) to remote regions was a problem" and that in this respect, "the ability to model the transport, scavenging and transformation of SO_2 and the production, transport and scavenging of $SO_4^=$ is still in its infancy". Thus, the challenge to COSAM was to test, using an expanded remote region sulphur data set, whether the models' performance in simulating transport to remote regions had improved after three years and to understand why variations between models and observations occurred. A 3rd conclusion was that "differences between model results reflect mainly the different treatments of the precipitation scavenging processes as well as differences in the hydrological parameters used to parameterize the scavenging".

The objectives of COSAM were to compare the ability of current models to simulate the spatial/temporal distribution of sulphate aerosols and to use an enhanced set of observations to accomplish this. The latter required a special effort undertaken by the global aerosol data centre (WMO/Global Atmospheric Watch [GAW] program) in Ispra, Italy to assemble all available ground level data on sulphates and its gaseous precursors, the use of a global data base on ^{210}Pb deposition in Grenoble, France and the use of an extensive set of aircraft vertical profile measurements of sulphates and related species at regionally repres-

entative locations on the periphery of the North American sulphur source region. In this paper, we describe the COSAM experiment: its design, the models and highlights of the results and conclusions. Companion papers address details of comparisons with regional sulphur budgets (Roelofs et al., 2001) and vertical distributions (Lohmann et al., 2001). Details of the COSAM experimental design and complete results can be found at the following website http://www.msc-smc.ec.gc.ca/armp/COSAM.html.

2. Model description

A brief summary of the models participating in COSAM is given in Table 1. A more detailed discussion can be found in Lohmann et al. (2001). 11 models participated, 3 of which are general circulation models (GCMs) generating their own winds, and 8 are chemical transport models (CTMs) that use prescribed analyzed winds. It should be emphasized that CC and GD in this study are nudged to analyzed winds but are dynamic models that can be run as climate models. GD uses the same physics as GB but imported-oxidant chemistry and is run using analyzed winds. It is therefore classed as a CTM. Furthermore, the dry deposition schemes of the two models are different. Due to considerable confusion in terminology regarding the definition of GCM and CTM, we emphasize that for this study the sole criterion for classifying a model as GCM or CTM is whether or not analyzed meteorological fields based on observations drive the model.

Clouds and chemistry play an important rôle in sulphur modeling. The complexity of the treatment of sulphur chemistry varies considerably. Models GB and CB have a full chemistry module which generates the precursors OH, H_2O_2, O_3 and NO_3 within the model while the rest of the global models rely upon importing climatological means of at least some of these variables or their precursors from outputs of other CTMs that are running internally-generated-oxidant. In what follows, we use the terminology internally-generated-oxidant chemistry and imported-oxidant-chemistry to clearly distinguish between these two methodologies. The regional model HA used an empirical conversion rate of SO_2 to $SO_4^=$ based on solar zenith angle and hence latitude and time of year (Christensen, 1997). The parameterization of clouds in the models are either prognostic or diagnostic utilizing the available meteorological parameters in the models.

3. Experimental design

Considering the complexity of comparing many models, an attempt was made to keep things simple. In addition, the design was shaped by the need to understand why differences occur. For GCMs, the recommended model run period was 3 to 5 years. In practice, only one model (GA) met this standard. For CTMs, the recommended model evaluation period was January 1993 to December 1995 with a preferred sub-period of July 1993 to June 1994. This period was chosen because there were many high quality routine observations of S compounds at remote stations in the Arctic, North Atlantic, eastern North America and Europe as well as numerous intensive field campaigns. In practice CTM, simulation periods ranged from 1 to 3 years. One model (CD) was included even though it ran only the $^{222}Rn/^{210}Pb$ option (for 1997/98) because it had run in previous inter-comparisons. Differing run times is a practical limitation imposed by available resources of the participants. It adds an uncertainty to the interpretation of results. However, it was felt that the value of broad participation in this intercomparison outweighed the drawbacks of variable run time. When considering differences between models and drawing conclusions, sensitivity to duration of a simulation were considered and are mentioned in the text.

Two run types were undertaken.

(i) A base run for sulphur compounds (SO_2, $SO_4^=$, DMS, MSA) with the following prescribed emissions.

(1) Anthropogenic S-emissions for 1985. GEIA 1B (Benkovitz et al., 1996).

(2) Monthly $1^\circ \times 1^\circ$ DMS emissions generated from gridded ocean surface DMS concentrations (Kettle et al., 1999), Liss-Merlivat air–ocean exchange parameterization and ECMWF (European Centre for Median Range Weather Forecasting) winds (see below for details).

(3) Volcanic emissions on a $3.75^\circ \times 3.75^\circ$ grid from Graf et al. (1997) and Spiro et al. (1992).

Munksgaard – Tellus Series B

Table 1. *Brief summary of sulphur models submitted for the COSAM exercise (see also Lohmann et al., 1999)*

Model code	Model name	Investigator	Simulation interval	Horizontal resolution	Vertical levels	Meteorology	Clouds	Ref.
GA	GISS	Koch	3 years	4° × 5°	9	generated	prognostic	Koch et al. (1999)
GB	ECHAM4-UU	Roelofs	2 years	3.75° × 3.75	19	generated	prognostic	Roelofs et al. (1998)
GC	CCCma	Lohmann	15 months	3.75° × 3.75	22	generated	prognostic	Lohmann et al. (1999)
GD	ECHAM4-MPI	Feichter Land Kjellstrom	7/93 to 6/94	2.81° × 2.81	19	nudged to ECMWF	prognostic	Feichter and Lohmann (1999)
CA	TOMCAT	Bridgeman Law	6/93 to 12/94	5.6° × 5.6°	31	ECMWF	diagnostic	Law et al. (1998); Giannakopoulos et al. (1999)
CB	KNMI/IMAU	Jeuken Dentener	1/93 to 12/93	3.75° × 5°	19	ECMWF	diagnostic	Dentener et al. (1999)
CC	MIRAGE	Easter	7/93 to 6/94	2.81° × 2.81	24	nudged	prognostic	Ghan et al. (2001)
CD	IMPACT	Bergmann	3/97 to 2/98	2° × 2.5°	46	GEOS	diagnostic	Penner et al. (1998)
CE	GOCART	Chin	7/93 to 6/94	2° × 2.5°	20	GEOS	diagnostic	Chin et al. (2000)
CF	NCAR	Rasch	9/92 to 12/95	1.8° × 1.8°	26	GEOS	diagnostic	Rasch et al. (2000a)
HA	DEHM	Christensen	12/92 to 12/95	150 km	12	ECMWF	prognostic	Christensen (1997)

(4) Any other sulphur sources such as biomass burning or sea salt were not included.

(ii) An optional Rn^{222}/Pb^{210} run using prescribed Rn^{222} emissions, a Rn^{222} first order radioactive decay rate of 2.11×10^{-6} s^{-1} to produce Pb^{210}, no other removal of Rn^{222} and removal of Pb^{210} as if it were $SO_4^=$. Rn^{222} surface emissions were prescribed (Table 2) in accordance with those outlined in Jacob et al. (1997).

The monthly DMS emission distributions used in the COSAM exercise, and the way they are constructed, is described by Kettle et al. (1999). A 1×1 database of monthly DMS surface water concentrations is constructed from 15 617 point measurements. The emission distributions are calculated with a parameterization for the air–sea transfer velocity (Liss and Merlivat, 1986), using ECMWF wind fields analyzed by Trenberth et al. (1989) and a sea surface temperature dependence from Erickson et al. (1990). The resulting global DMS emission fluxes are about 2.8 and 1.4 Tg S per month for January and July, respectively, and 28.9 Tg S yearly.

For all compounds modeled, the following 10 results were reported for each model:

(1) Global budgets.

(2) Regional budgets. Four regional budget areas were selected, three in the major anthropogenic source regions of eastern North America, Europe and Southeast Asia as well as a Southern Ocean Biogenic Source Region (Fig. 1). The budgets were calculated for two layers (0 to 2.5 km and 2.5 km to the top of the domain). For details see Roelofs et al. (2001).

(3) Global distributions of seasonal mean mixing ratios in the lowest model layer and seasonal mean column burdens in the 0 to 1 km and total column layers.

(4) Seasonal (defined as winter December to February, etc.) mean and standard error of the daily mean mixing ratio of surface level SO_2, non-sea salt sulphate (nss-$SO_4^=$) and MSA at locations shown in Fig. 1 where regionally-representative, long-term surface observations were available.

(5) Pole to pole vertical transects for northern hemispheric summer (June to August) and winter (December to February) of mean and standard deviation of daily mean mixing ratios for the mid-Atlantic (longitude 30° W), mid-Pacific (longitude 160° W) and mid-North America (longitude 80° W).

(6) Vertical profiles of period mean mixing ratios off the east coast of Canada corresponding to the intensive aircraft observations made during the North Atlantic Regional Experiment (NARE) in July/August 1993 and a March/April vertical profile for North Bay Ontario, Canada (46.3° N; 79.5° W) where sufficient multi-year sampling was available to constitute a climatology. For details see Lohmann et al. (2001).

(7) For CTMs, the mean vertical profile of ^{222}Rn mixing ratios from 0 to 12.5 km altitude at 37.4° N, 122° W near San José, California for the period 3 to 16 June 1994 corresponding to aircraft observations (Kritz et al., 1998) made generally between the hours of 00 and 06 GMT (i.e., late afternoon) on 11 days in that period (CTMs provided profiles for the actual observation period while GCMs provided mean profiles for June).

(8) Annual mixing ratio of ^{210}Pb in the surface layer of the model (specify thickness) from 5° to 35° N latitude along a longitude band in India from 70° to 85° E.

(9) Gridded seasonal mean deposition of ^{210}Pb for: (i) total deposition (i.e., wet plus dry) and (ii) wet deposition (seasons: winter: December to February, etc.).

(10) Monthly mean and standard deviation of daily mean mixing ratios of ^{222}Rn and ^{210}Pb in surface air at 7 locations where long term air concentration measurements are available (Crozet 46.45° S, 51.85° E; New Amsterdam 37.83° S, 72.53° E; Dumont d'Urville 67.00° S, 142.00° E; Kerguelen 49.33° S, 70.38° E; Bombay 18.95° N, 71.92° E; Fribourg 46.80° N, 7.15° E; Summit 72.30° N, 38.00° W). Observations are from the

Table 2. *Radon emissions used in the optional model run*

Latitude	Longitude	^{222}Rn source strength (atoms cm^{-2} s^{-1})
70° 90° N and S	all	0
60° 70° N and S	all	0.005
60° S–60° N	oceans	0.005
60° S 60° N	land	~ 1.0[a)]

[a)] Adjust ^{222}Rn source strength from land so that global source of ^{222}Rn is 72 mol yr^{-1}. The reason for this is because land area may vary between models.

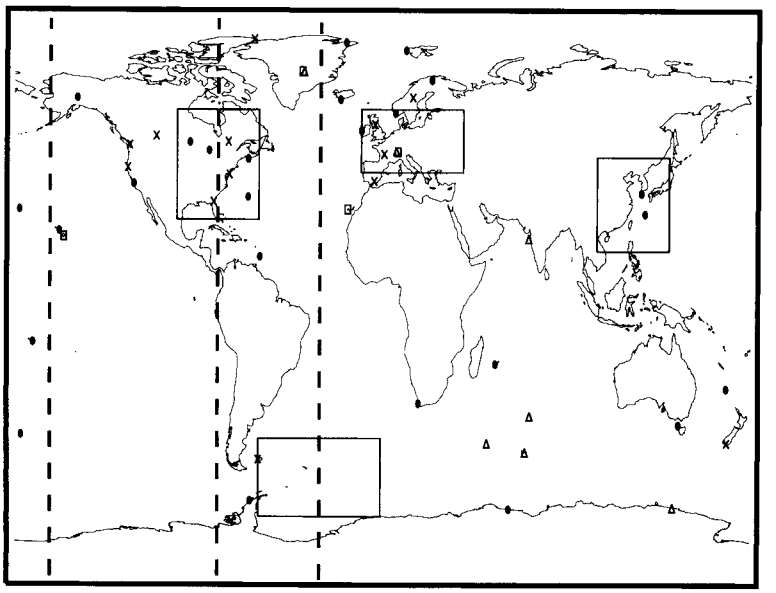

Fig. 1. A map showing (a) locations of sites where surface observations of sulphur compounds were available for comparison with models (black dots: mandatory for all models to provide data [see * sites in Table 3]; x's mark optional surface sites for models to provide data and squares mark elevated mountain sites), (b) location of ^{222}Rn and ^{210}Pb measurement sites marked as triangles, (c) three longitudinal transects (heavy dashed lines)along which seasonal means of all species measured were provided and (d) boxes delineating areas in which mass budget information was reported (see results in Roelofs et al., 2001).

data center in Grenoble (Melieres, personal communication).

The above model products were chosen to enable a comparison of models with each other and with observations on different scales. A major effort in this study was dedicated to assembling and quality controlling observational data against which model predictions could be tested. Because much uncertainty is involved in comparing a point surface observation with a spatially-averaged model output, the strategy was adopted to use regional budgets to describe model performance within source regions and only to use sites that are sufficiently distant from major anthropogenic sources that a point measurement is indeed a reasonable estimate of a model grid-average mixing ratio (Fig. 1). The regional budget results are analyzed in detail in a companion paper by Roelofs et al. (2001).

Surface-based observations of sulphur species were compiled by the WMO GAW aerosol data center by J. Wilson and F. McGovern. In order to utilise consistent measurements, where similar collection and analysis techniques were used, data from large-scale networks were preferred. However, the nature of scientific research means that a number of key sites are operated on a single site basis. Data availability and quality were also considered. Table 3 lists the surface sites selected. The networks and single site operations that agreed to supply data for the project were:

Networks

- Air Ocean Chemistry Experiment (AEROCE), University of Miami, USA.
- Canadian Air and Precipitation Monitoring Network (CAPMON), Environment Canada Toronto, Canada.
- US Department of the Energy Network, (DOE), University of Miami, USA.
- Co-operative Programme for Monitoring and Evaluation of the Long Range Transport of Air Pollutants in Europe (EMEP), Norwegian Institute for Air Research.
- Interagency Monitoring of Protected Visual Environments (IMPROVE), USA.

Table 3. *Summary of source of ground level data*

(I) Boundary of source regions

Site	Country	Lat.	Long.	Alt. (m)	MSA	SO_2	Group
Jergul*	Norway	69.4	24.6	255		√	EMEP
Skreaadalen*	Norway	58.82	6.72	475		√	EMEP
Bredkälen	Sweden	63.85	15.33	404		√	EMEP
Eskdalemuir	UK	55.32	−3.2	243		√	EMEP
La Crouzille	France	45.83	1.27	497		√	EMEP
La Cartuga	Spain	37.2	−3.6	720		√	EMEP
Denali NP*	USA	63.72	−148.97	658		√	improve
Ester	Canada	51.67	−110.2	707		√	CAPMON
Exp. Lakes*	Canada	49.65	−93.72	369		√	CAPMON
Algoma*	Canada	47.03	−84.37	411		√	CAPMON
Chapais	Canada	49.82	−74.97	381		√	CAPMON
Brigantine	USA	39.45	−74.43	5			improve
Okefenokee	USA	30.73	−82.12	38		√	improve
Pinnacles*	USA	36.48	−121.15	317		√	improve
Redwood	USA	41.55	−124.07	232		√	improve
Saturna	Canada	48.78	−123.13	178		√	CAPMON

(II) North Atlantic and Arctic sites

Site	Country	Lat.	Long.	Alt. (m)	MSA	SO_2	Group
Alert	Canada	82.47	−62.5	210	√		AES
Nord*	Greenland	81.43	−17.5	???		√	DRC
Spitzbergen*	Norway	78.9	11.88	474		√	EMEP
Heimaey*	Iceland	63.25	−20.15	100	√		U. Miami
Mace Head*	Ireland	53.33	−9.9	20	√		U. Miami
Kejimkujik*	Canada	44.43	−65.2	127		√	CAPMON
Bermuda*	UK	32.32	−65.27	30	√		U. Miami
Barbados*	UK	13.17	−59.43	3	√		U. Miami

(III) North Pacific Ocean sites

Site	Country	Lat.	Long.	Alt (m)	MSA	SO_2	Group
Cheju*	Korea	33.52	126.48	20	√		U. Miami
Okinawa*	Japan	26.92	128.25	23	√		U. Miami
Norfolk*	Australia	−29.08	167.98	20	√		U. Miami
Midway*	USA	28.22	−177.35	15	√		U. Miami
A. Samoa*	USA	−14.25	−170.58	25	√		U. Miami
Hawaii*	USA	21.33	−157.7	17	√		U. Miami

(IV) Southern hemisphere sites

Site	Country	Lat.	Long.	Alt (m)	MSA	SO_2	Group
Cape Grim*	Australia	−40.68	144.68	94			U. Miami
Chatham Is.*	N. Zealand	−43.92	−176.5	20			U. Miami
Invercargill	N. Zealand	−46.43	168.35	30			U. Miami
Reunion*	France	−21.17	55.83	60	√		U. Miami
Cape Town*	S. Africa	33.8	18.47	50			U. Miami
Palmer Station*	Antarctica	−64.92	−64.05	20	√		U. Miami
Mawson*	Antarctica	−67.6	62.5	20	√		U. Miami
Mt. Pleasant	UK	−51.75	−60	100			U. Miami

(*continued*)

Table 3. *(continued)*
(V) Elevated sites

Site	Country	Lat.	Long.	Alt. (m)	MSA	SO_2	Group
Izana*	Spain	28.3	−16.48	2367			U. Miami
Jungfraujoch*	Switzerland	46.55	7.98	3573		√	EMEP
Mauna Loa*	USA	19.53	−155.58	3397			U. Hawaii
Summit*	Greenland	73.3	−38.8	3190	√		C. Mellon U

The site list is comprised of optional sites for which modelled data may, or may not, be submitted and required sites, for which modelled data should be submitted. The "required sites" are indicated by a *. The site ID used in the list is that used by the original site-operating organisation. See Fig. 1.

Single sites

- Mauna Loa Observatory, University of Hawaii (UH), USA.
- Summit, Greenland, Université Joseph Fourier (UJF), Grenoble, France.
- Alert, Atmospheric Environment Service (AES), Canada.
- Nord, Greenland, Danmarks Miljoundersøgelsers (DMU).

Systematic observations of vertical distributions of the compounds modeled are scarce. We chose two locations in Canada on the periphery of the North American source region where sufficient aircraft observations of $SO_4^=$ and its gaseous precursors SO_2 were available to provide a good estimate of the mean vertical profile of mixing ratio in the atmosphere. In addition, ancillary measurements of the aqueous phase oxidants ozone and hydrogen peroxide as well as cloud properties were available to test the models. Evaluation of model performance in this regard is discussed in detail in the companion paper by Lohmann et al. (2001).

4. Results and discussion

In Subsections 4.1–4.7, detailed results are presented of comparison of models based on 7 specific diagnoses. These compare the models' ability to simulate parameters related to: (i) annual global budgets of S, Rn^{222} and Pb^{210}, (ii) seasonal mean regional budgets of S, (iii) seasonal mean latitudinal variation in the northern hemisphere of the zonal distribution of three column sulphur properties, (iv) seasonal mean vertical distributions of S parameters along a mid-Atlantic transect, (v) ground based $SO_4^=$ and SO_2 mixing ratios at regional and remote sites and (vi) Rn^{222} vertical profiles and remote ground level mixing ratios. Finally in Subsection 4.8, an explanation is offered for sources of discrepancies between models and observations that is generally consistent with these 7 tests.

4.1. *Global budgets*

All models ran the same emissions scenario and there was good agreement between the reported global emissions of DMS, SO_2, SO_4 and ^{222}Rn. However, a comparison of the annual mean global atmospheric mass of ^{222}Rn, ^{210}Pb, SO_2 and $SO_4^=$ (Fig. 2) showed considerable differences between models. This parameter is subject to all of the atmospheric processes affecting a substance after it is emitted. The clearest difference was for ^{210}Pb (Fig. 2a), the particulate end product of gaseous ^{222}Rn decay. Models GB, GC and GD were higher than the rest by at least 30%. This result is an indication of the relative ability of the models to scavenge particulate matter from the atmosphere. The constant decay rate of Rn and its inertness with respect to wet and dry deposition leave only scavenging processes to affect the model outcome. When variable oxidation and wet/dry deposition processes of the gaseous precursors (i.e., DMS and $SO_4^=$ are involved, differences in the model-predicted particulate end product (i.e., $SO_4^=$ and MSA) disappear in the added variance of the model results (Fig. 2b). This is due to added variance associated with the gaseous precursors (DMS, SO_2) undergoing wet and dry removal and variable oxidation rates whereas ^{222}Rn is only subject to a constant radioactive decay rate (half-life 3.82 day). Thus, models GB, GC and GD

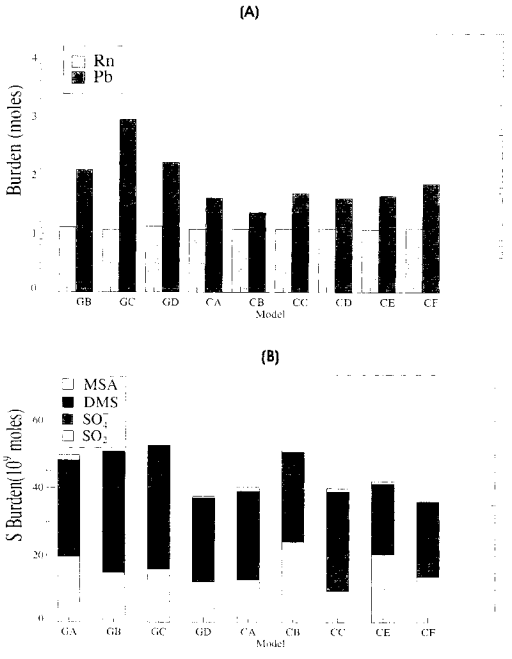

Fig. 2. Comparison of annual average total mass (burden) of (a) ^{222}Rn and ^{210}Pb and (b) total atmospheric S and its components in the global atmosphere.

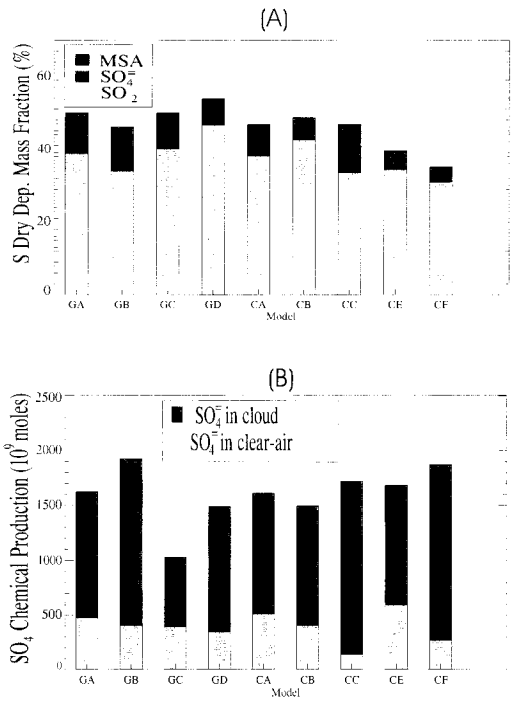

Fig. 3. Comparison of global model performance with respect to dry and wet removal of SO_x species: (a) the fraction of total S emission that is dry deposited annually in the model domain in the form of various sulphur components. The rest is wet removal. (b) Comparison of annual mean chemical production rates of $SO_4^=$ from oxidation of gaseous precursors in clear air and within clouds.

scavenge particulate matter from the atmosphere 30% less effectively than the other global models.

In Fig. 2b, the composition of atmospheric sulphur predicted by each model is also compared. Atmospheric sulphur is dominated by gaseous SO_2 and $SO_4^=$ aerosols. DMS and MSA constitute less than 15% of the total (Fig. 2b). The 10 models are consistent in predicting that on a global mean basis atmospheric $SO_4^=$ is slightly more abundant than SO_2 (50 to 70% of SO_x).

The relative performance of models on a global basis to remove sulphur by wet and dry deposition and to produce $SO_4^=$ in clear air is shown in Figs. 3a, b. There is some variation in the fraction of total sulphur deposited that is scavenged by wet and dry processes (Fig. 3a). The dry deposited fraction ranges from 36 to 54%. With the exception of model GC, there is little variation in the total annual chemical production of $SO_4^=$ by clear air and in-cloud oxidation of gaseous precursors (Fig. 3b). For the majority, its rate ranges from 1500 to 1900 Gmoles yr^{-1} Model GC was much lower at 1000 Gmoles yr^{-1}. The fraction of $SO_4^=$ production occurring in-cloud ranges from 78% in-cloud for CA to 91% for model CC.

The atmospheric residence time of sulphur compounds was calculated by dividing the annual domain average burden of a sulphur species by the sum of its sinks (chemical destruction, dry deposition and wet removal). Generally, the residence time of particulate $SO_4^=$ (3.6–7.5 days) was longer than for SO_2 (1.3–3.1 days). The lifetime of DMS which is largely determined by reaction with OH and to a lesser extent with NO_3 radicals ranged from 1 to 3.9 days with most models predicting a lifetime of close to 2 days. Model GB was much higher at a DMS residence time of 3.9 days while model CA was lowest at 1 day. Consistent with this is that model GB had fractionally less clear air $SO_4^=$ production (i.e., less OH and hence higher DMS lifetime) than the median

of the group while model CA had fractionally more clear air production than the median of the group (Fig. 3b).

The two models running internally-generated-oxidant chemistry had very different DMS lifetimes (GB 3.9 days, CB 2 days). This indicates that in marine areas of high DMS emissions OH concentrations predicted by the two models differ considerably. In CB, non-methane hydrocarbon chemistry is represented by the Carbon Bond Mechanism 4 (CBM-4), while in GB only the CO yield from oxidation of NMHC are accounted for. The effect of including NMHC chemistry is a decrease of simulated lower tropospheric OH over the continents and an increase over oceans (e.g., Houweling et al., 1998). This may partly explain the difference between the DMS lifetimes in these two models.

4.2. *Regional budgets*

Highlights of a detailed analysis of the regional sulphur budgets for the major pollution source regions eastern North America, Europe and south-eastern Asia on a seasonal basis (Roelofs et al., 2001) are as follows.

(i) Simulation of vertical transport of sulphur species in the source regions is highly variable between models, especially in summer.

(ii) Dry deposition removal of SO_2 and sulphate in the source regions varies by a factor of 3 between models. This is much more variable than for the global scale.

(iii) Wet deposition is of relatively little importance in the regional budget of SO_2, but a dominant factor in that of $SO_4^=$. Simulated wet deposition rates for sulphate range over a factor of 4, whereas one model stands out even more with a very high wet deposition efficiency. Global budget results (Subsection 4.1) show that this conclusion is valid on a larger scale although there is less variance between models for the larger global domain.

(iv) In most models in all regions, about 50% of the sulphate resides above 2.5 km altitude.

(v) Export of SO_2 and $SO_4^=$ from polluted source regions to cleaner areas varies greatly between models showing differences up to an order of magnitude in summer. However, variabilities in the separate SO_2 and sulphate exports are somewhat anti-correlated resulting in less difference in SO_x export between models.

There was considerable variation in SO_x export between models from region to region and season to season (Fig. 4). The greatest seasonality in fractional export was in Europe, while the greatest variability between models occurred in eastern North America and southeast Asia rather than Europe. In summer, the GCM GA was less efficient in transporting SO_x from eastern North America and southeast Asia than the others.

4.3. *Latitudinal variations in zonal distributions of sulphur compounds*

Insight into the performance of the models in horizontally transporting, vertically dispersing, and oxidizing sulphur compounds has been gained by comparing model predictions of three parameters: (i) the column burden of SO_x, (ii) the

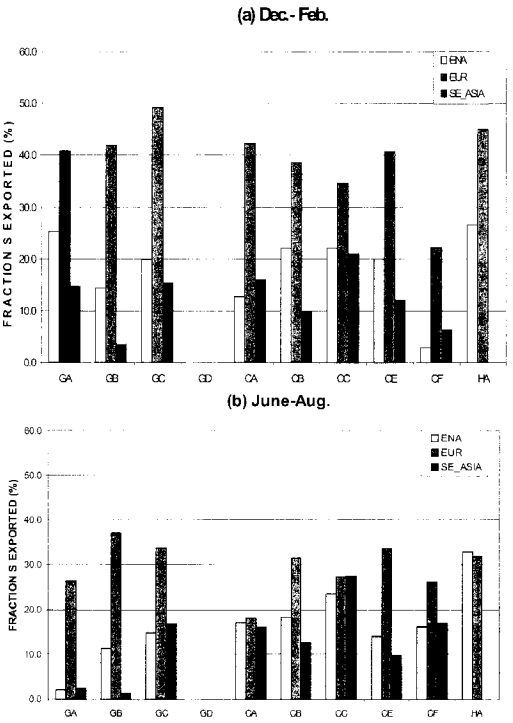

Fig. 4. A comparison of model performance in exporting anthropogenic sulphur from the three major source regions on Earth in (a) winter and (b) summer. The fraction of total emissions in the source regions of eastern North America (ENA), the European EMEP region (EUR) and southeast Asia (SE-ASIA) is shown. A result for model GD was not available (Roelofs et al., 2001).

fraction of total column SO_x that is in the first kilometer and (iii) the fraction of total column SO_x that is SO_2. The distribution of each of these parameters for a zone or latitude band around the Earth in the northern hemisphere is compared for winter and summer in Figs. 5, 6. Results for HA were not available for latitude band 0 to 15°N since this model has a northern hemispheric sub-domain in which results near the lower latitude boundary are not realistic. It should also be emphasized that variance of the parameter distribution (indicated by height of boxes) may be related to model resolution. In principle, more highly resolved models such as HA, CD, CE and CF will tend to have higher variance than low resolution models such as GA and CA (Table 1).

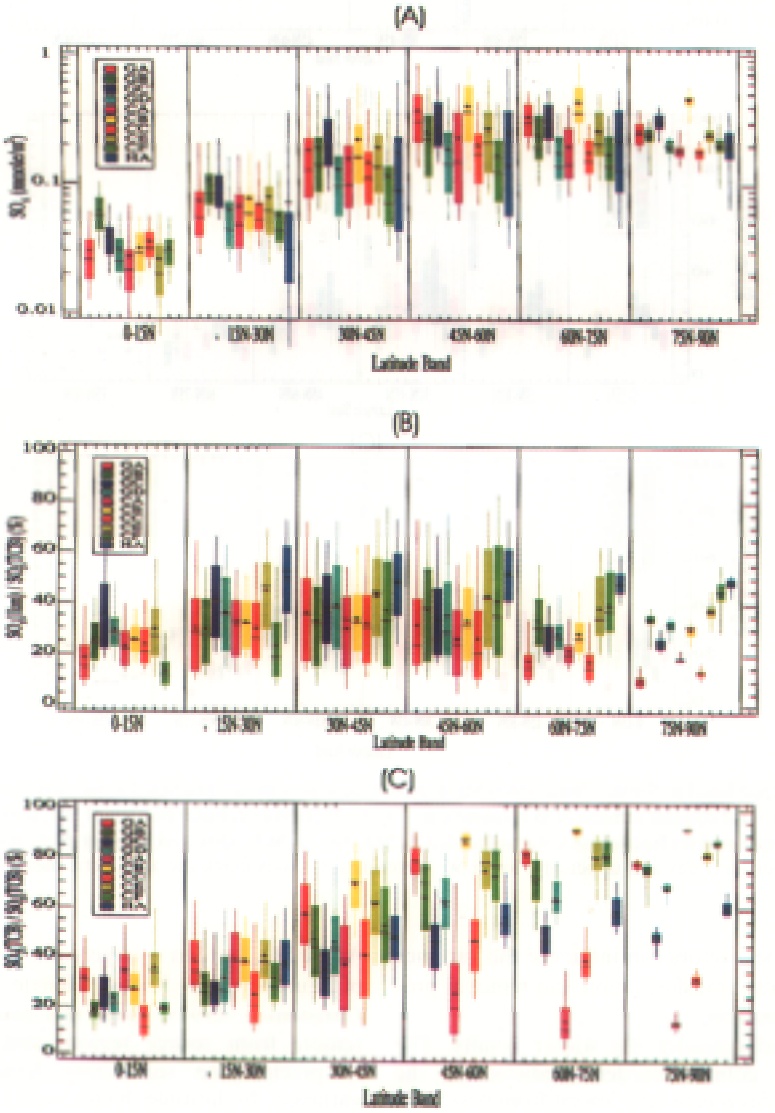

Fig. 5. By latitude band in the northern hemisphere, a comparison of model predicted zonal distributions in winter (December–February) of (a) column burden of SO_x (mmole m^{-2}), (b) fraction of column burden of SO_x in the first kilometer of the atmosphere and (c) fraction of column burden of SO_x that is SO_2. Box and whisker plots represent medians, upper and lower quartiles and upper and lower 95 percentiles. Crosses mark the arithmetic mean.

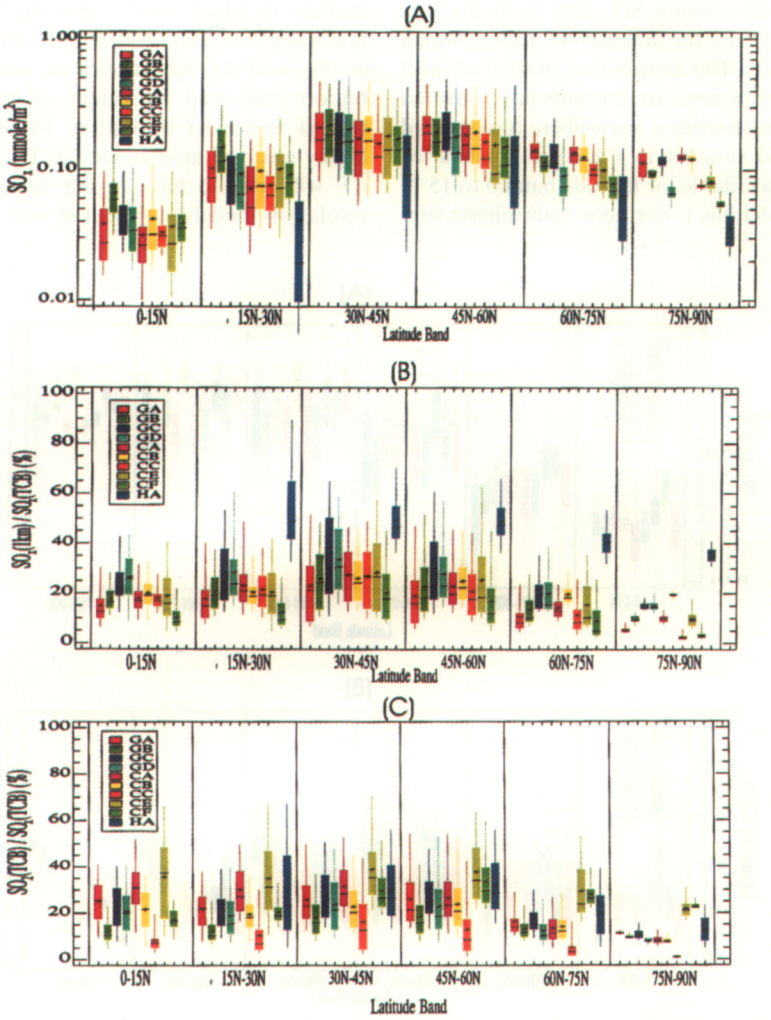

Fig. 6. By latitude band in the northern hemisphere, a comparison of model predicted zonal distributions in summer (June–August) of (a) column burden of SO_x (mmole m^{-2}), (b) fraction of column burden of SO_x in the first kilometer of the atmosphere and (c) fraction of column burden of SO_x that is SO_2. Box and whisker plots represent medians, upper and lower quartiles and upper and lower 95 percentiles. Crosses mark the arithmetic mean.

However, other factors can influence the variance such as the way transformation and removal processes are simulated.

Let us first consider the winter results. The median SO_x column burden predicted by the models (Fig. 5a) is generally lowest from 0 to 30°N (0.02 to 0.09 mmole m^{-2}) and highest north of 45°N (0.15 to 0.45 mmole m^{-2}). The greatest variance between model medians is in the low to mid-latitudes and the least in the high Arctic. The Arctic SO_x burden is largely due to transport out of Europe and Russia (Barrie et al., 1989; Christensen, 1997). Thus, this reservoir is most remote from source regions and least subject to precipitation scavenging; hence, the lower variance. In latitude bands north of 45°N, the internally-generated-oxidant chemistry transport model CB consistently calculates higher SO_x column burden relative to the other models. The rest of the models are divisible into a low and a

high SO_x burden group with the GCMs and one CTM(CE) in the high group and GC and the remaining CTMs in the low group.

In the source region (30 to 60 N) in winter, the median fraction of column SO_x burden that is in the first kilometer does not vary consistently with latitude. It ranges from 20 to 48% (Fig. 5b). HA, the high resolution sub-hemispheric model, tends to have more SO_x in the lowest levels than the other models. It will be shown later in Subsection 4.5 that HA is the best in matching seasonal mean surface concentrations of SO_2 and $SO_4^=$ in winter. Moving northward in latitude shows differences in models increasing until the fraction ranges from 10 to 50% in the Arctic region (>75 N). Models GA, CA and CC are lowest while HA is highest.

In winter, the median fraction of total column burden SO_x that is unoxidized SO_2 (Fig. 5c) increases from low to high latitudes and is most variable in the mid- to high latitudes. Models CA and CB represent lower and upper bounds, respectively. They range from 40 and 70%, respectively at 30–45 N to 12 and 92% north of 60 N. Thus, there are great differences in the way models oxidize SO_2 and because OH concentrations are low, the differences are in the models' aqueous phase oxidation parameterizations. HA which matches observations well predicts 60% in the three latitude bands between 30 and 90 N.

It is noteworthy that in the winter months in the remote Arctic, which receives most of its pollution from Eurasia (Barrie et al., 1989; Christensen, 1997), most models perform consistently in transporting SO_x to the remote northern latitudes (Fig. 5a) but vary greatly in how they disperse that SO_x in the vertical (Fig. 5b) and how they apportion it between SO_2 and $SO_4^=$ (Fig. 5c).

Let us now consider the results for the summer. Median SO_x burden (Fig. 6a) tends to peak in the mid-latitudes (30–60 N) in contrast to the winter situation when the burden at high latitudes were as high as those at mid-latitudes. Model CB which was generally higher than the rest in winter is now in the middle of the group. The hemispheric model HA is consistently lower than the rest. In the mid-latitudes, variance between models is less than in winter while at the high latitudes it is higher.

The fraction of total column SO_x in the lowest 1 km is less in summer than in winter and tends to be lowest in the high latitudes. As in winter, the hemispheric model HA is much higher than the rest. In other words, it confines much more SO_x to the lower atmosphere than the other models. This model does not simulate vertical convective mixing. This is likely a drawback in summer but not in winter. The difference is most pronounced in summer when convection is strongest.

As expected from atmospheric photochemistry, the fraction of total column SO_x that is SO_2 (Fig. 6c) is much lower in summer than in winter. Furthermore, it decreases with increasing latitude while in winter the opposite was true. There was much less variance in this parameter in summer than in winter. This could be expected since oxidation of SO_2 is faster in summer, and in all the models the oxidation is sufficiently fast that most SO_x exists as $SO_4^=$. North of 30 N, models CE, CF and HA are consistently higher than the rest while model CC is lower. In winter, model CA replaces model CC as the lowest. The chemical transport model CB which has internally-generated-oxidant chemistry and which was highest in winter (i.e., low SO_2 oxidation and/or removal) was in the middle of the group in summer.

These results present us with a dilemma. Model HA, which matches surface level observations reasonably well, consistently retains more SO_x in the lowest 1 km than the other models. It should be emphasized that there is a bias in the fraction of total column SO_x in the lowest 1 km associated with the top of model HA being lower (6 km) than that of the other models (>10 km). However considering that ~60% of the atmospheric mass lies below 6 km and that mixing ratios are much higher below 6 km than above, this bias will be less than 20%. In Model HA, considerable attention has been paid to obtaining accurate numerical solutions of advection equations. A combination of a pseudo spectral method with a Forester filter gives a very accurate solution to the advective transport equation (Dabdub and Seinfeld, 1994). It also has a good vertical diffusion scheme that mixes pollutants in the planetary boundary layer. Another, unique feature of HA is that SO_2 transformation is empirically parameterized as a function of solar zenith angle. If HA is indeed correct, it indicates that the global models need to improve their chemical transformation of SO_2 and their

parameterization of transport and vertical dispersion in moving material beyond source regions.

4.4. *Longitudinal profiles of sulphur parameters along the mid-Atlantic*

Further insight into the relative performance of the models can be gained by comparing vertical cross sections of various parameters along longitude 30 W (see Fig. 1). In the northern hemisphere, the mid-latitude portion of this transect is downwind of the eastern North American source region in the westerlies and the northern latitudes (>70 N) receives pollution mainly from Eurasia particularly in winter. Figs. 7, 8 show results for December to February for SO_x and the fraction of that SO_x that is SO_2, respectively. As mentioned above, the higher resolution limited area model HA has been particularly well tested and validated in Europe and the northern latitudes of the lower troposphere (Christensen, 1997) and can serve as somewhat of a benchmark in winter when deep convection (which it does not simulate as well as GCMs) does not play a large rôle in vertical mixing. The SO_x mixing ratio has two maxima. One north of 50 N associated with anthropogenic sources and a smaller one in the southern high latitudes associated with biogenic DMS emissions in the southern hemispheric summer.

Models differ greatly in the SO_x amount that they put into the northern troposphere in the northern hemispheric winter (Fig. 7). The area of the troposphere covered by isolines 0.30 nmole/mole-air and greater varies by a factor of 10. Models GA, GC, CB and CE maintain more SO_x in the winter troposphere than the other models. This is consistent with an over-prediction of ground level SO_2 in winter (see Subsection 4.5). Differences lie not in the ground level concentrations but in the areal extent of the anthropogenic sulphur in the atmosphere. Variations in export of SO_x from Europe or North America (Fig. 4) are not sufficient to explain an order of magnitude variation in spatial extent displayed in Fig. 7. Model HA yields realistic ground level concentrations and vertical distributions of SO_x in winter (Christensen, 1997). The fact that model HA does not disperse anthropogenic SO_x in the vertical as readily as the lower resolution models suggests that vertical diffusion is a major source of variance.

On the mid-Atlantic vertical transect in winter, variances in SO_x distributions between models (Fig. 7) are not correlated to oxidization of SO_2 indicated by SO_2/SO_x fractions (Fig. 8). Models GA, CB, CE and CF have SO_2/SO_x fractions that are greater than 75% over large areas of the northern troposphere while the rest are generally below 65% over most of the northern latitudes.

An analysis of regional sulphur budgets (Roelefs et al., 2001) led us to the conclusion that the dominant cause of model-to-model differences for the three northern hemispheric source regions is the representation of cloud processes: aqueous-phase sulphate production rates, wet deposition efficiency and vertical transport efficiencies. The same likely holds for transport beyond the source regions with one additional source of variance, namely efficiency of horizontal transport.

In northern hemispheric winter, there is a maximum oxidation of DMS emitted from high latitude southern polar oceans which leads to aerosol $SO_4^=$ peaks. Some models have this feature and some do not. A comparison of the two internally-generated-oxidant chemistry models GB and CB is particularly interesting. On the basis of global annual sulphur budgets (Subsection 4.1), it was concluded that CB was more efficient in oxidizing DMS than GB (respective DMS tropospheric lifetime of 2 versus 3.9 days). This is consistent with results in Fig. 7 with CB having a marked southern hemispheric SO_x peak at ~60 S and GB a less distinct one. Another process that plays a role in the production of $SO_4^=$, from DMS is cloud chemistry and removal. This may also be a source of difference between the modeled $SO_4^=$ distributions.

A comparison of results for the mid-Atlantic longitudinal profile of aerosol sulphate mixing ratio in the northern hemispheric summer period is shown in Fig. 9. At this time of year remote from source regions, $SO_4^=$ is the dominant contributor to SO_x (Fig. 6c). With the exception of model GA, there is consistency between models in simulating a maximum in the mid-Atlantic downwind of eastern North America. Models are divisible into two groups based on their movement of sulphate aerosol aloft and poleward into the troposphere. GA, GB, GC, CA, CC and CF produce considerable $SO_4^=$ aloft while GD, CB, CE and HA confine it more to the mid- to lower troposphere. Another difference is concentrations in the atmospheric boundary layer at high latitudes

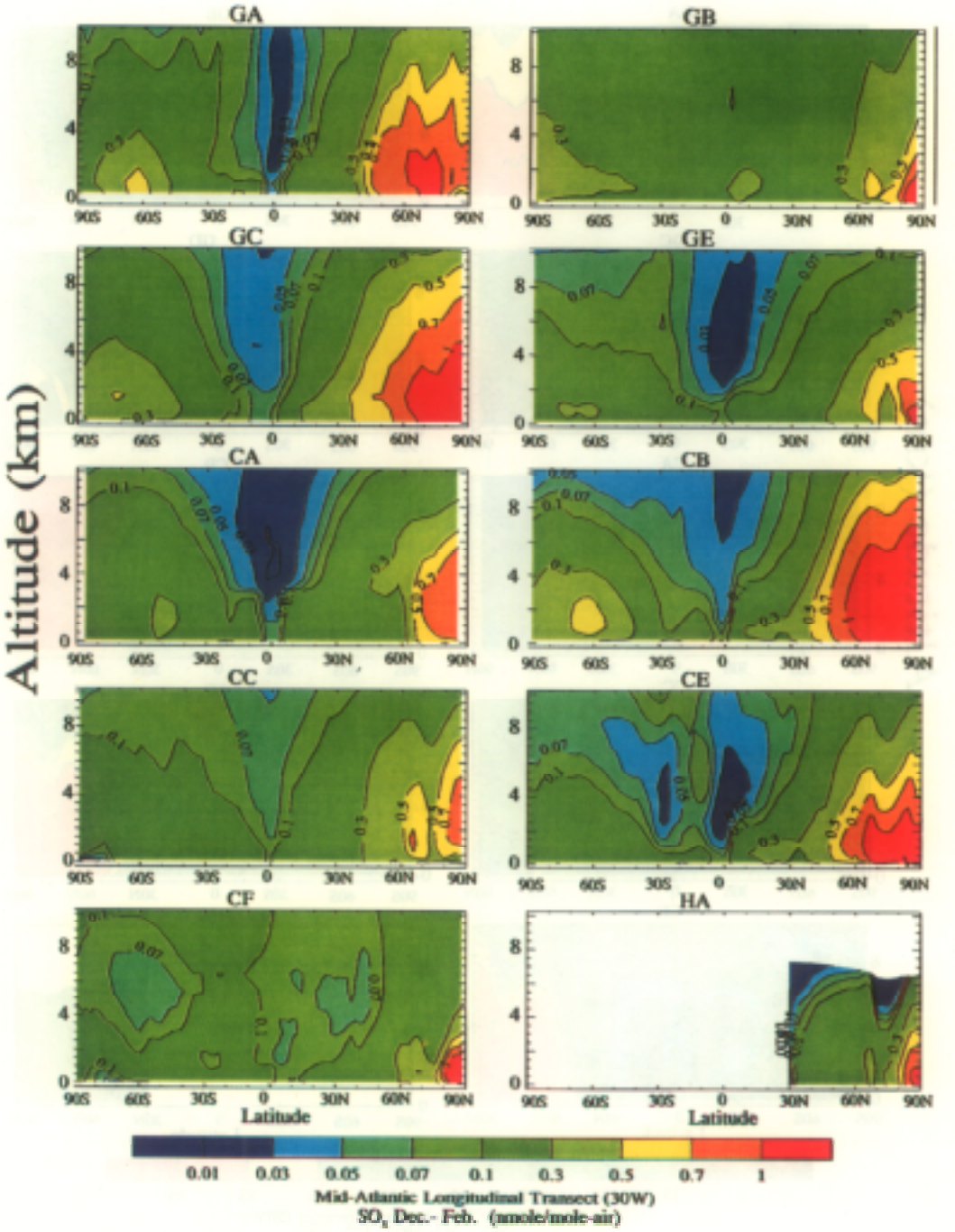

Fig. 7. A longitudinal profile comparison of model simulated mean SO_2 mixing ratio (nmole/mole-air) along a mid-Atlantic transect at 30°W (Fig. 1) for the northern hemispheric winter (December–February).

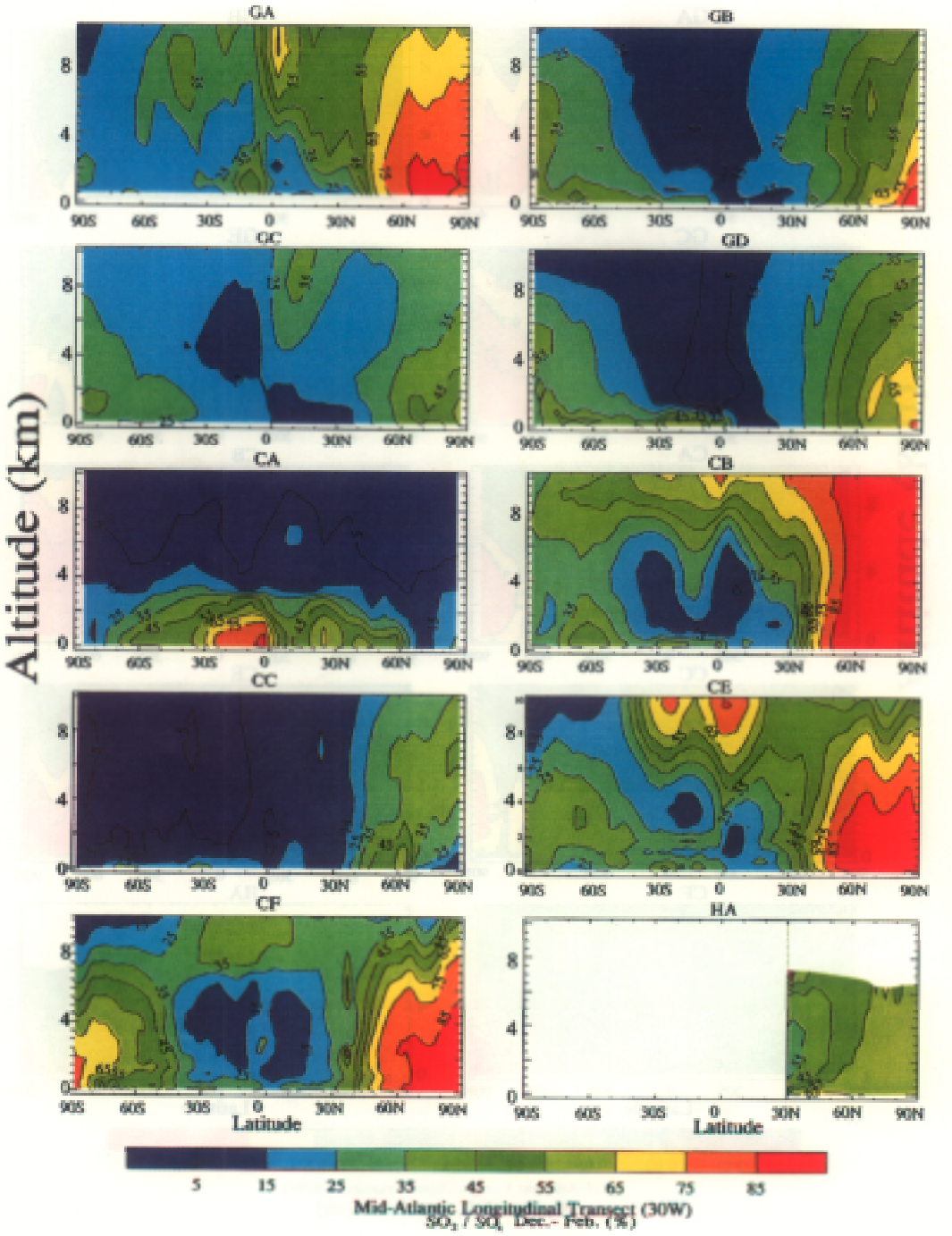

Fig. 8. A longitudinal profile comparison of model simulated mean SO_2/SO_x molar ratio (%) along a mid-Atlantic transect at 30°W (Fig. 1) for the northern hemispheric winter (December–February). This corresponds to the SO_2 mixing ratio results in Fig. 7.

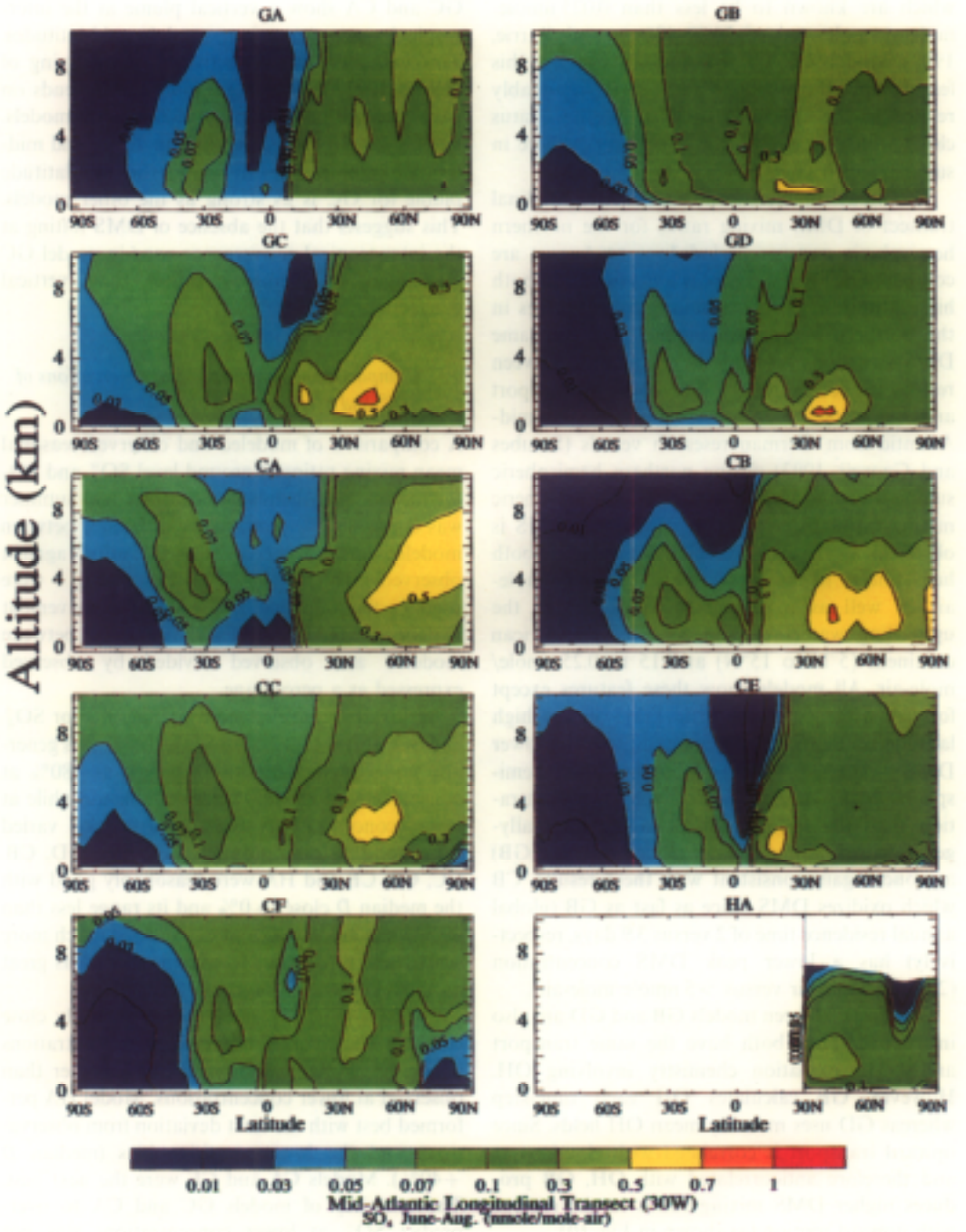

Fig. 9. A longitudinal profile comparison of model simulated mean $SO_4^=$ mixing ratio (nmole/mole-air) along a mid-Atlantic transect (30°W) for the northern hemispheric summer (June–August).

which are known to be less than 0.025 nmole/mole-air poleward of 70°N (Sirois and Barrie, 1999). Models CC, CF, CE and HA simulate this feature while the others do not. This is presumably related to the ability to produce marine stratus cloud which dominates the lower troposphere in summer north of 70°N.

The model predicted mid-Atlantic longitudinal transect of DMS mixing ratios for the northern hemispheric summer period June to August are compared in Fig. 10. There is a maximum in both high latitude regions originating from sources in the northern oceans. All models used the same DMS emissions so that the variations between results are determined by differences in transport and oxidation. DMS observations in the mid-Atlantic from German research vessels (Staubes and Georgii, 1993) during northern hemispheric summer have measured surface level atmospheric mixing ratios from 52°N to 52°S. Peak DMS is observed at the extreme high latitudes of both hemispheres in the range 0.5 to 1.5 nmole/mole-air as well as a secondary maximum in the up-welling waters off the coast of the African continent (5°N to 15°N) at 0.15 to 0.25 nmole/mole-air. All models show these features except for CA which has very little DMS in the high latitude southern hemisphere and generally lower DMS everywhere. Model CF has a southern hemispheric peak but clearly also lower in concentration than the rest. Contrasts in the internally-generated-oxidant chemistry models (CB and GB) are once again consistent with these results. CB which oxidizes DMS twice as fast as GB (global annual residence time of 2 versus 3.9 days, respectively) has a lower peak DMS concentration (2 nmole/mole-air versus >5 nmole/mole-air).

Contrasts between models GB and GD are also instructive. They both have the same transport and DMS oxidation chemistry involving OH. However, GB calculates OH each time-step whereas GD uses monthly mean OH fields. Since upward transport is correlated with cloud cover and therefore anticorrelated with OH, GB produces higher DMS mixing ratios in the regions with upward motion (as shown in Fig. 10).

The vertical dispersion of DMS into the upper troposphere that is evident for all models in Antarctica in Fig. 10 is presumably driven by circulation around the Antarctic continent in southern hemispheric winter. All models except GC and CA show a vertical plume at the inter-tropical convergence zone and in mid-latitudes. This is caused by convective cloud pumping of this relatively insoluble gas aloft and depends on parameterization of deep convection in the models. Results for Rn also show the equatorial and mid-latitude plumes. In this case, the mid-latitude plume for GC is as strong as the other models. This suggests that the absence of DMS lofting at the inter-tropical convergence zone in model GC is related to chemistry rather than vertical convection.

4.5. *Comparison with ground level observations of $SO_4^=$ and SO_2*

A comparison of modeled and observed seasonal mean mixing ratios of ground level $SO_4^=$ and SO_2 for the northern hemispheric winter and summer was conducted by plotting the difference between modeled and observed mixing ratios against observed mixing ratios. The sites in Fig. 1 were used. In the following discussion, it is convenient to define the parameter D as the difference between modeled and observed divided by observed expressed as a percentage.

Let us first consider the winter results for $SO_4^=$ and SO_2 (Figs. 11, 12). For $SO_4^=$, the models generally under-predicted with D as low as −80% at concentrations above 0.8 nmole/mole-air while at lower concentrations their performance varied from good to poor. Models GA, GB, GD, CB, CC, CE, CF and HA were reasonably good with the median D close to 0% and its range less than 30% while model GC and CA showed much more scatter and a tendency to over-predict (D as great as 150%).

For SO_2 (Fig. 12), results were generally close to — or less than — observed at concentrations above 1.5 nmole/mole-air and much higher than observed at lower concentrations. Model HA performed best with the least deviation from observations and the lowest positive bias (median D +40%). Models CA and CF were the next best. The tendency of models GC and CA to over-predict $SO_4^=$ at lower concentrations was not compensated by an under-prediction of SO_2. This clearly indicates that transport and removal rather than oxidation are sources of the deviation from observed.

In Figs. 13, 14, the results for northern hemi-

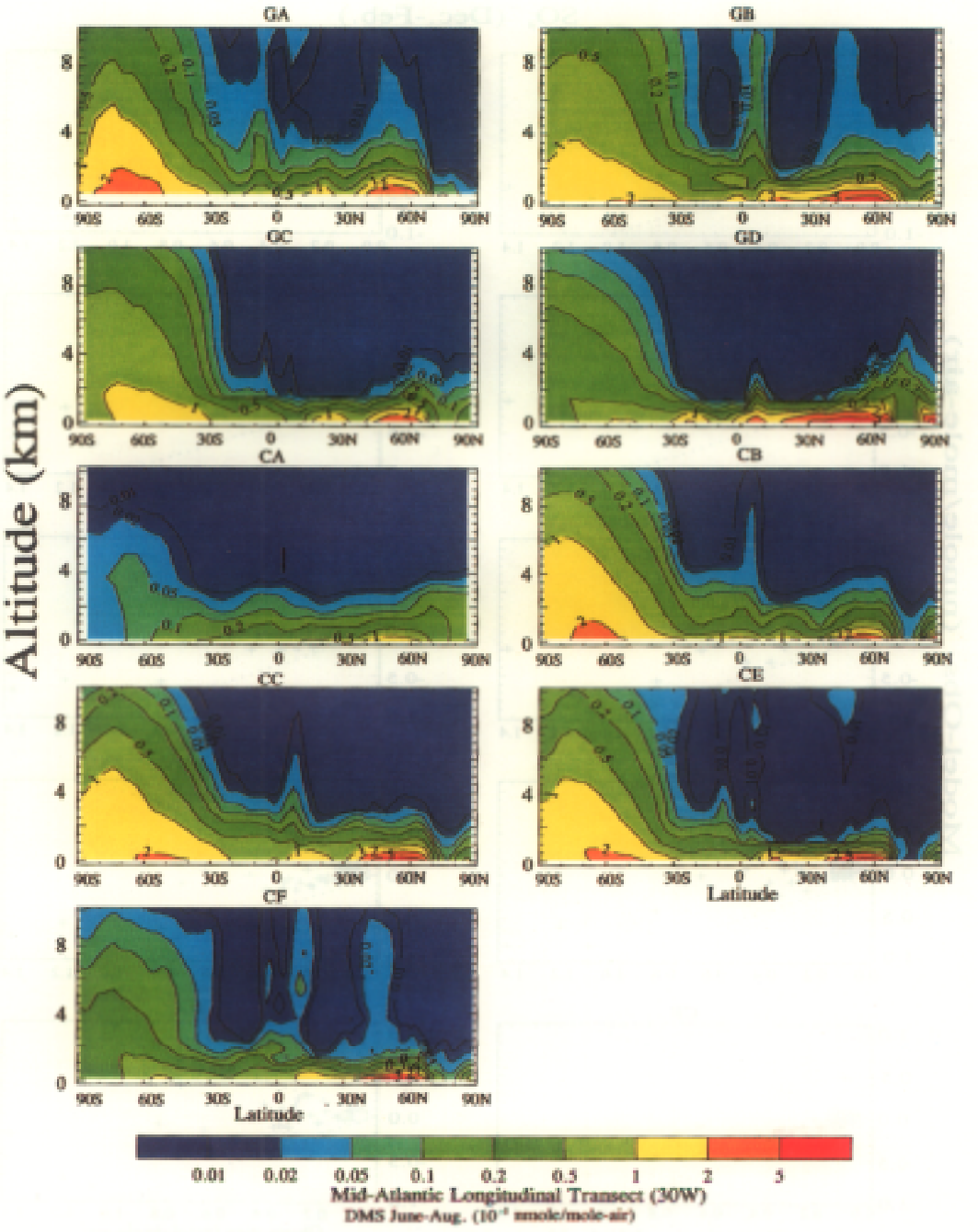

Fig. 10. A longitudinal profile comparison of model simulated mean DMS mixing ratio (units of 0.1 nmole/mole-air) along a mid-Atlantic transect at 30°W for the northern hemispheric summer (June–August). Corresponds to the results for $SO_4^=$ in Fig. 9.

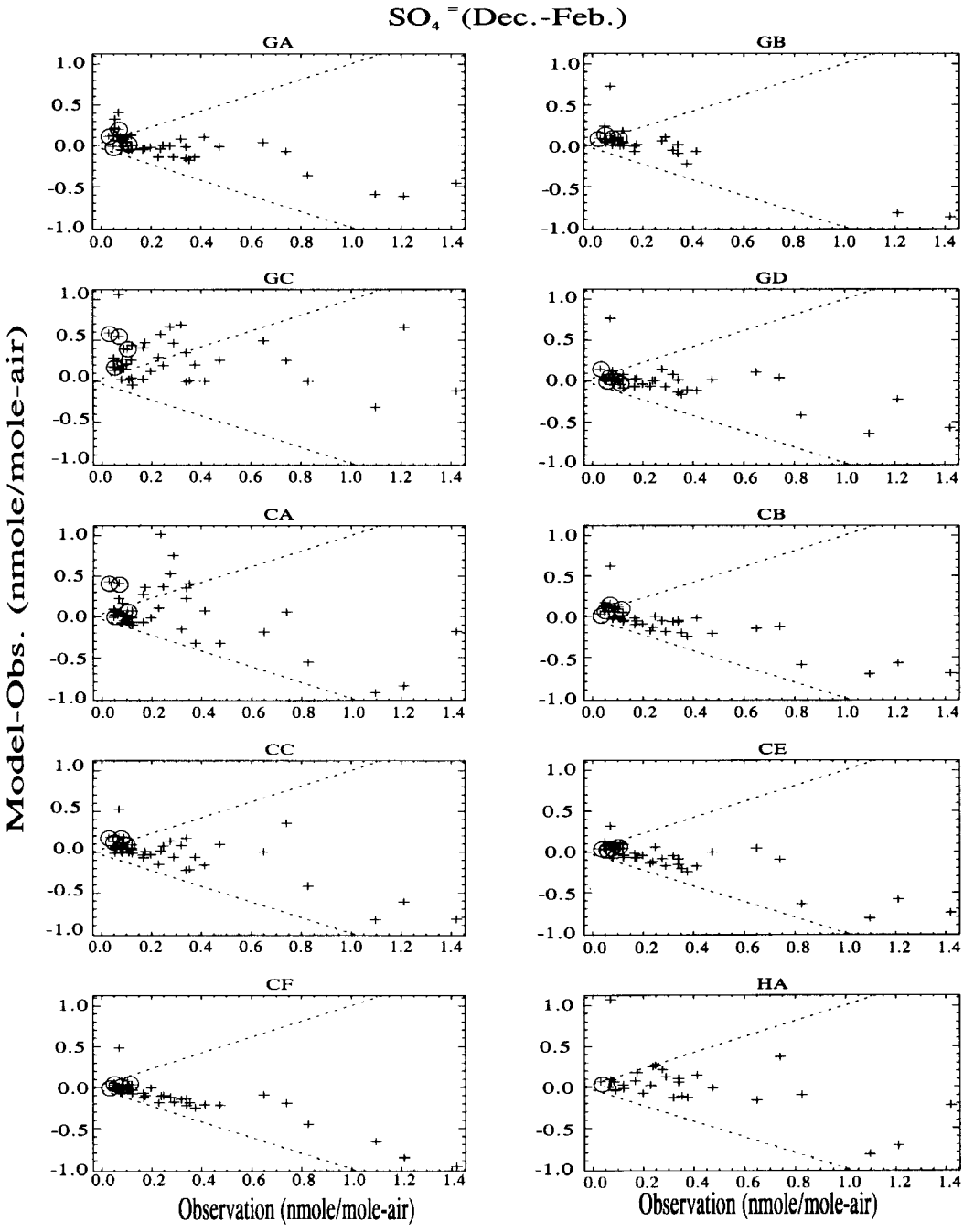

Fig. 11. For $SO_4^=$ in the northern hemispheric winter (December February), a comparison of modeled and observed seasonal mean mixing ratios at ground level at regionally representative locations (Fig. 1) around the world. The difference between seasonal mean modeled and observed mixing ratio is plotted versus observed mixing ratio. The horizontal line at 0 represents perfect agreement between model and observations.

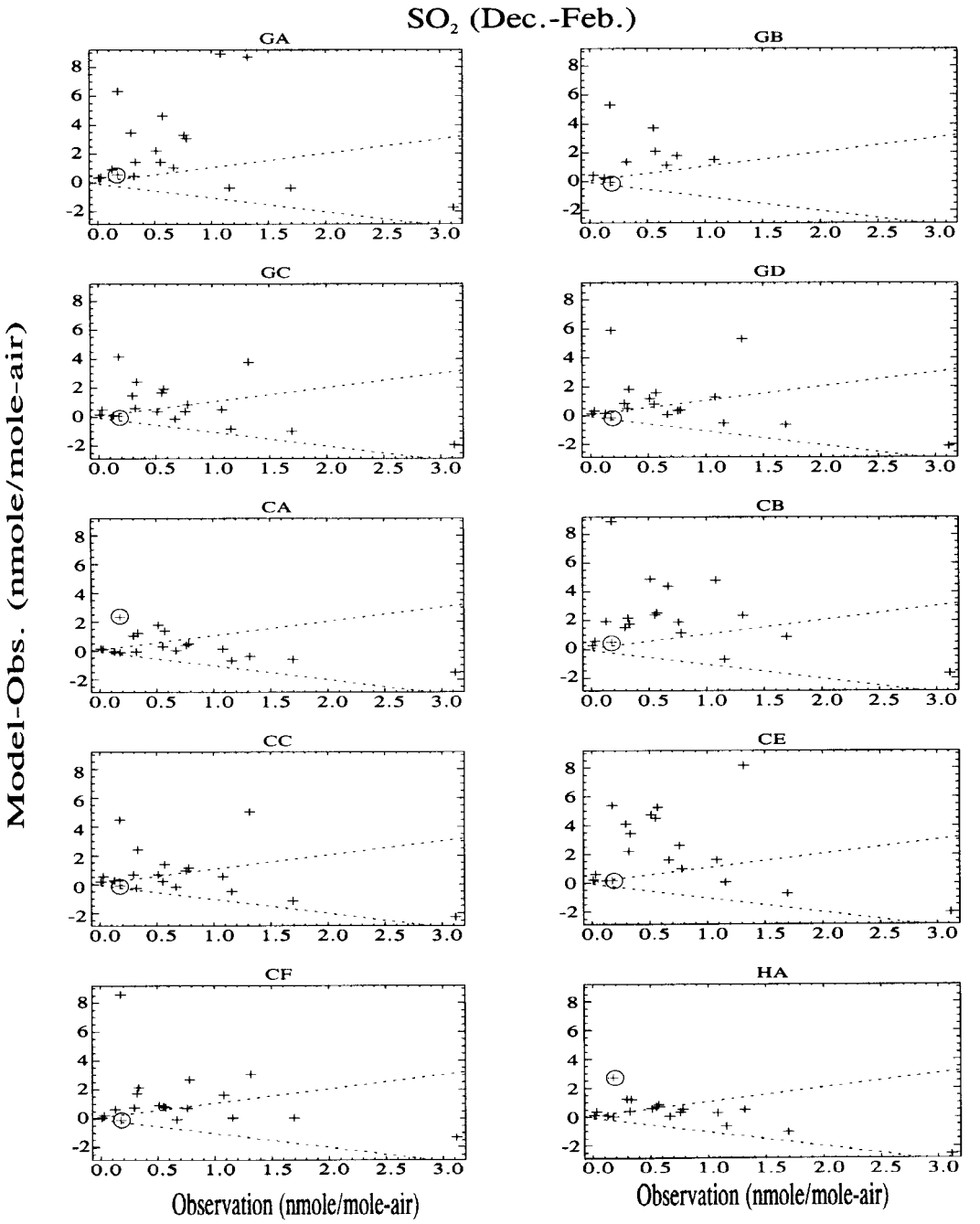

Fig. 12. For SO_2 in the northern hemispheric winter (December February), a comparison of modeled and observed seasonal mean mixing ratios at ground level at regionally representative locations (Fig. 1) around the world. The difference between seasonal mean modeled and observed mixing ratio is plotted versus observed mixing ratio. The horizontal line at 0 represents perfect agreement between model and observations.

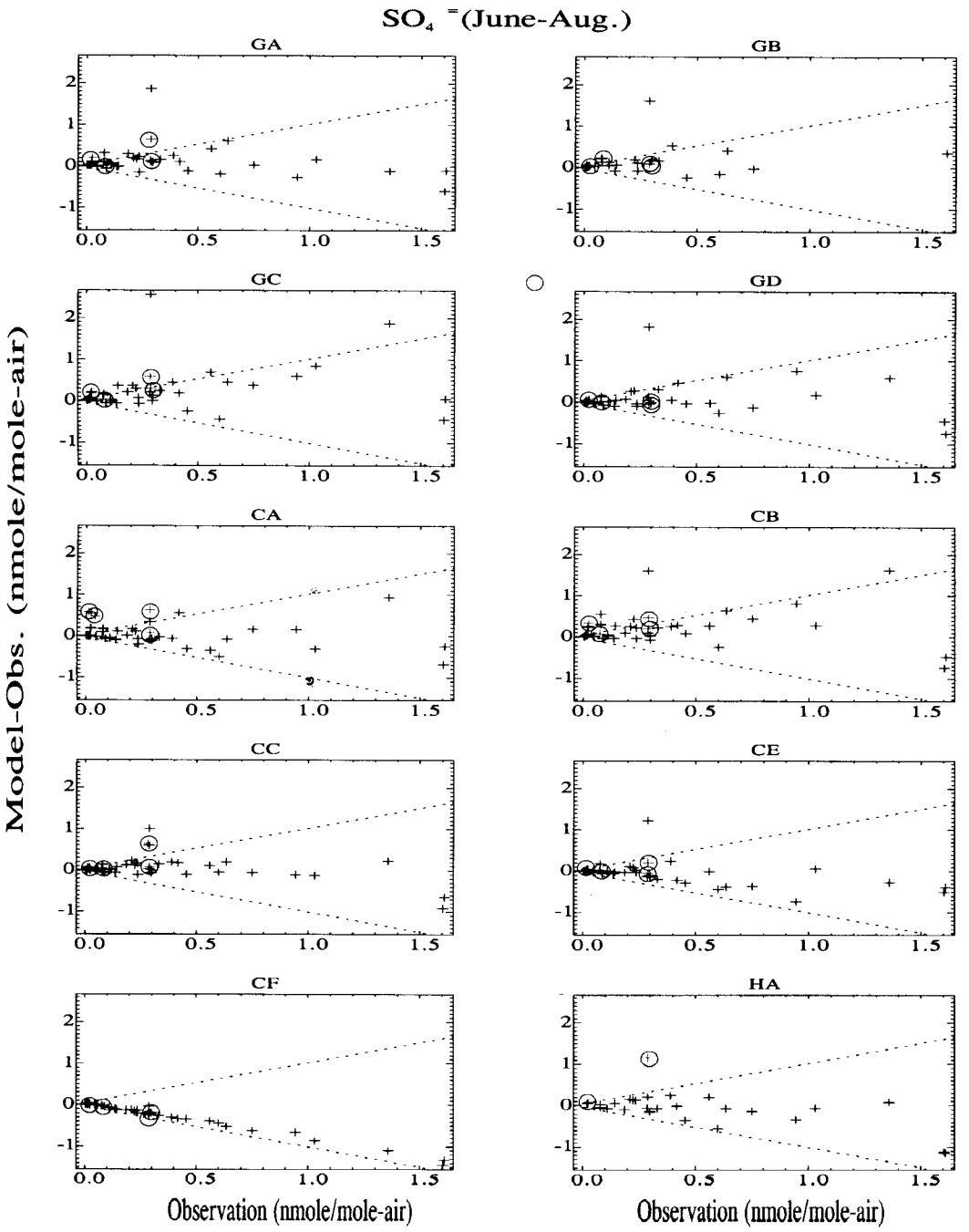

Fig. 13. For $SO_4^=$ in the northern hemispheric summer (June–August), a comparison of modeled and observed seasonal mean mixing ratios at ground level at regionally representative locations (Fig. 1) around the world. The difference between seasonal mean modeled and observed mixing ratio is plotted versus observed mixing ratio. The horizontal line at 0 represents perfect agreement between model and observations.

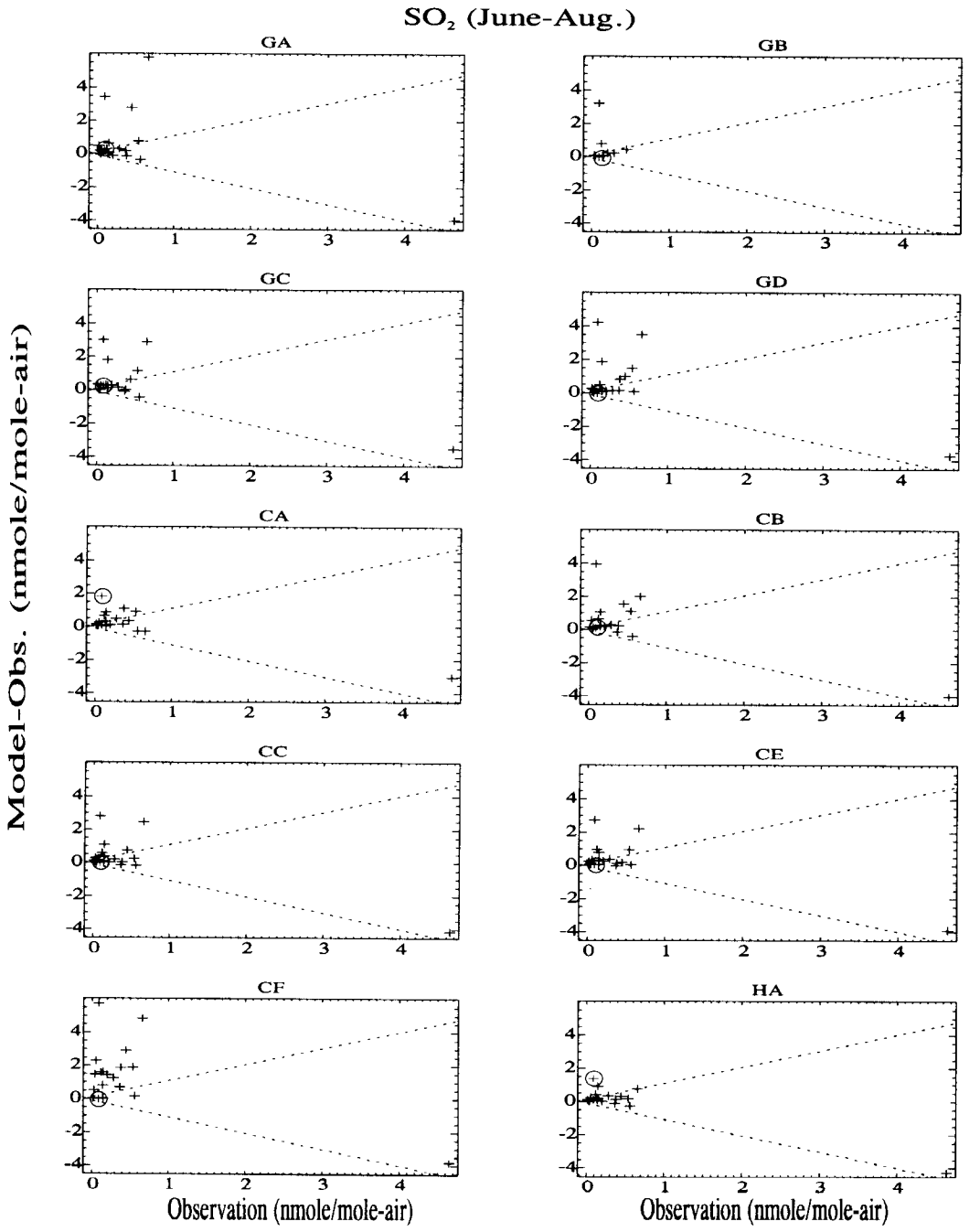

Fig. 14. For SO_2 in the northern hemispheric summer (June August), a comparison of modeled and observed seasonal mean mixing ratios at ground level at regionally representative locations (Fig. 1) around the world. The difference between seasonal mean modeled and observed mixing ratio is plotted versus observed mixing ratio. The horizontal line at 0 represents perfect agreement between model and observations.

spheric summer are compared. For $SO_4^=$ (Fig. 13), model performance was much better than for the winter period (Fig. 11). Models GA, GB, GD, CA, CC and HA showed no systematic bias with observations (i.e., mean $D = 0$) over the whole data range. Furthermore, scatter about the observations was less than 50% and in the case of model CC less than 20%. Other models show considerable systematic bias. GC and CB had an average bias of D from 70 to 80% while CF showed a remarkably consistent negative bias of 70%. As in the winter months, all models but HA tended to over-predict SO_2 (Fig. 14) by 20 to 50%. Since SO_2 oxidizes more rapidly in summer than in winter, the only SO_2 observations above detection limit are those close to source regions. Hence, there are fewer points in Fig. 14 than in Fig. 13. Model CF showed very large scatter for SO_2 in contrast to its results for $SO_4^=$ but this time a positive bias (D approximately 400%).

The general tendency to over-predict SO_2 while predicting $SO_4^=$ reasonably well suggests that there is a problem with unrealistically high long range transport out of source regions in the models. One possible source of bias is in the representativeness of the 1985 SO_2 emissions for which the observations are available (mainly representing the late 1980s to mid-1990s). Most SO_2 observations are on the periphery of Europe and N. America. An examination of emissions differences would explain the models being high by 20 to 40%. This is generally not enough to explain the discrepancy evident in Figs. 12, 14.

Data from 4 elevated mountain sites are included and plotted as circled crosses in Figs. 11 to 14 (Izana, Spain 2367 m asl; Jungfraujoch, Switzerland 3573 m asl; Mauna Loa, USA 3397 m asl; Summit, Greenland 3190 m asl). There was no systematic difference between these and other sites in the models' ability to simulate observations. However only 1 of the 4, Jungfraujoch had SO_2 as well as SO_4. More routine observations at elevated locations are needed.

In summary, a comparison of model-predicted surface-level mixing ratios of sulphur compounds at regionally representative monitoring sites around the world proved to be very useful particularly because they were chosen to be on the periphery of source regions and in more remote areas downwind of source regions. Models tended to predict seasonal mean $SO_4^=$ mixing ratios in winter and summer better than they did those of SO_2. On average, they were within 20% of $SO_4^=$ observations with a few notable exceptions while they over-predicted SO_2 by factors of 2 or more. Furthermore in winter at sites with high concentrations (i.e., those near source regions), many models tended to under-predict $SO_4^=$ concentrations. The limited area model HA performed best by matching both parameters within 20%.

4.6. *Rn vertical profiles near San José, California*

A comparison of models with observations of the mean vertical profile of ^{222}Rn mixing ratios near San José, California from 0 to 12.5 km altitude is shown in Fig. 15. The observations are based on aircraft soundings in late afternoon/evening (00 to 06 GMT) on 11 days for the period 3 to 16 June 1994 (M. Kritz, 1998). It should be emphasized that the results for the GCMs and the CTMs CB and CD do not correspond exactly to the weather conditions in which these observations were taken. The GCM results represent a climatological prediction for the period while CB and CD results are for the same time of year but different years (1993 and 1997, respectively). Also, this is a coastal location subject to land–sea wind circulations. Thus, the observed profiles result from both vertical and horizontal transport, and the global models cannot be expected to reproduce these circulations well. The outcome is that while the models perform very well in the matching observations between 4 and 10 km altitude, they tend to deviate from observations in a systematic pattern below 4 km. The tendency is to under-predict from 2 to 4 km just above the planetary boundary layer and to over-predict near the ground. They are not adequately dispersing Rn into the troposphere above.

Another noteworthy aspect of comparisons is the inability of any of the models to adequately capture the upper tropospheric increase (relative to the mid-troposphere values) in the observed Rn concentrations. Such upper tropospheric increases were a marked feature of both the individual as well as the mean profiles in the San José area (Kritz et al., 1998) and probably resulted from strong convective transports of Rn-rich air from the Asian boundary layer to the upper troposphere, followed by rapid eastward movement at elevated altitude (Kritz et al., 1990). In general,

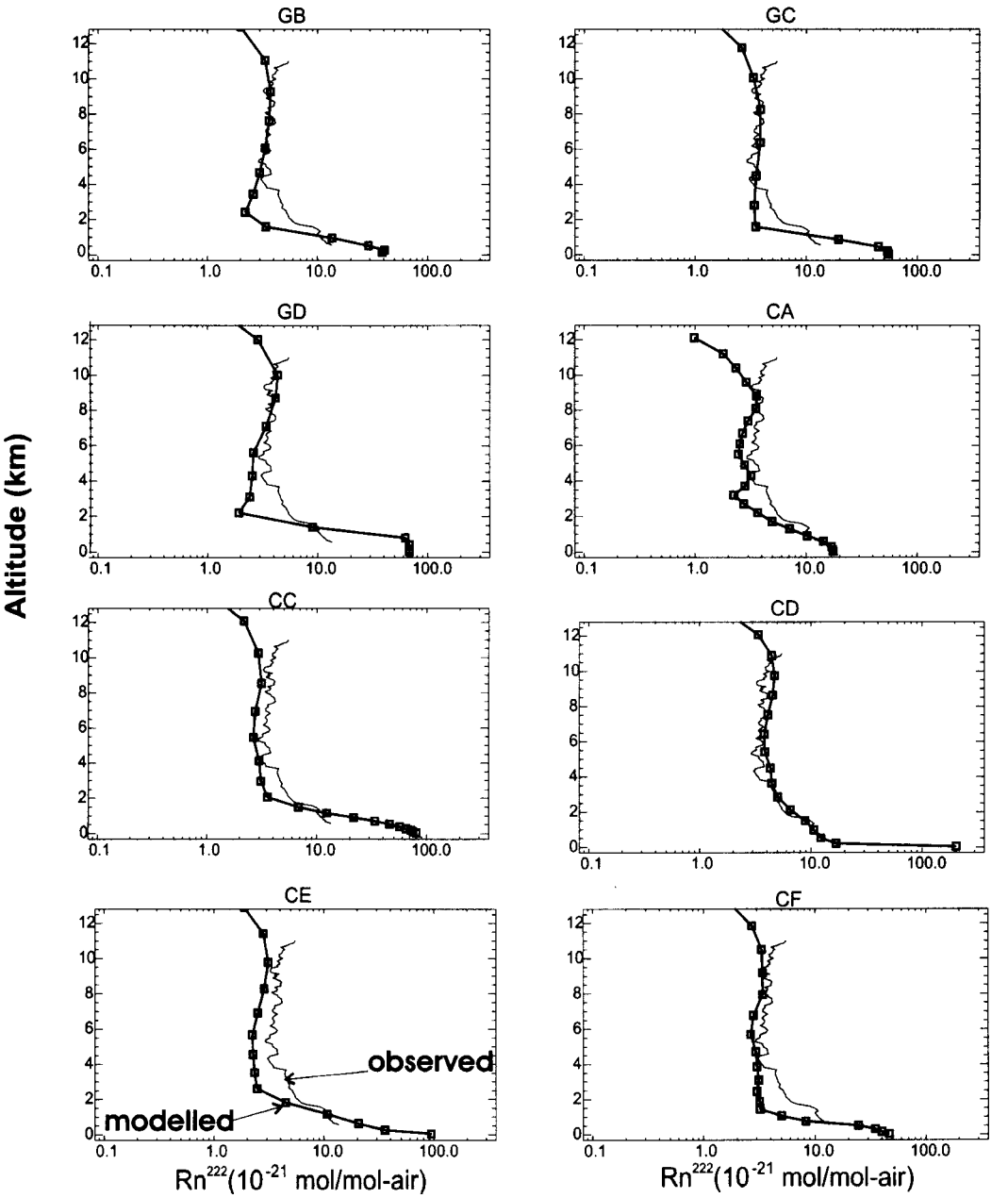

Fig. 15. A comparison of modeled and observed mean vertical profiles of ^{222}Rn at 37.4 N, 122 W near San José, California based on aircraft observations on 11 days in the late afternoon/evening (00 to 06 GMT) for the period 3 to 16 June 1994 (M. Kritz, personal communication).

boundary layer mixing parameterizations schemes are not adequately dispersing Rn into the troposphere above.

4.7. *Monthly ^{210}Pb and ^{222}Rn at remote locations stations*

It should be emphasized that in the following comparisons of observed and modelled results in remote areas for the ^{222}Rn and ^{210}Pb that all models used the same prescribed emissions (Table 2) consistent with those previously used in a global model intercomparison (Jacob et al., 1997). Those emissions were low and constant regardless of season for the latitude band from 60 to 70 in both hemispheres.

4.7.1. Remote Southern Ocean marine sites. Monthly atmospheric mixing ratios of ^{222}Rn and ^{210}Pb have been observed on the remote marine islands of New Amsterdam (37.83 S, 72.53 E), Kergelen (49.33 S, 70.38 E) and Crozet (46.45 S, 51.85 E). These islands are far from the main continental source of ^{222}Rn in South Africa (Fig. 1). A typical result for this group is shown in Fig. 16 for New Amsterdam Island. Mixing ratios are at least an order of magnitude lower compared to a continental source such as Bombay or Freiberg (0.2 to 0.7×10^{-21} nmole/mole-air ^{210}Pb; 0.6 to 1×10^{-21} nmole/mole-air ^{222}Rn). All models except CF consistently predict ^{222}Rn mixing ratios that are high by a factor of 2 to 10 but have the right seasonal cycle. For ^{210}Pb, they predict mixing ratios that are high by a factor of 2 to 10 with no seasonal variation in agreement with observations. Model CF does not simulate the seasonal cycle and tends to be more variable from month to month. Thus, either modeled transport of continental emissions from the southern African continent to these islands is too strong or emissions of ^{222}Rn are too high. The first explanation is consistent with conclusion drawn above for SO_x transport from source regions to remote areas of the northern hemisphere.

Results at the Antarctic site Dumont Durville (67.00 S, 142.00 E) are consistent with the lower latitude southern ocean sites. Except in the months of January and February, all models except CF over-predicted ^{222}Rn by factors of 2 to 10.

In a detailed comparison of versions of models GD and CB with ^{222}Rn observations (Dentener et al., 1999), it was concluded that differences between modeled and observed mixing ratios were due to uncertainties in ECMWF winds used to drive the model, the assumed ^{222}Rn emission and sub-grid parameterizations of vertical transport. As in the COSAM run, both models tended to over-predict mixing ratios at remote southern ocean marine sites. They performed better in shorter range transport from Australia to Cape Grim, Tasmania and from eastern North America to Bermuda. Since in the above COSAM results, discrepancies with observations appeared with GCMs as well as these CTMs, sub-grid parameterization of mixing must be a significant source of model error relative to input winds.

4.7.2. Summit, Greenland. Summit (72.30 N; 38.00 W) on Greenland is an elevated (3210 m asl) site at the top of the Greenland plateau. Measurements of ^{222}Rn and ^{210}Pb were made there very recently as part of the joint European/American over-wintering project. A comparison of modeled and observed ^{222}Rn and ^{210}Pb at this site showed that models systematically over-predict ^{222}Rn mixing ratios by a factor of 2 to 10 while for ^{210}Pb some are consistently higher by a factor of 1.5 to 5 (GB, GD, CA, CB, CE) and some are lower (CC and CF). Model HA is closest to observed but significantly over-predicts ^{222}Rn in winter. None of the models reproduce the observed seasonal cycle of ^{222}Rn. The inability of models to simulate the transport of ^{222}Rn (the gaseous precursor of aerosol ^{210}Pb) to Greenland is consistent with their inability to match ground level SO_2 mixing ratios in remote regions (Figs. 12, 14). Another source of uncertainty is the assumed ^{222}Rn emissions (Table 2).

4.8. *Insights into sources of model uncertainty afforded by the 7 tests*

In the northern hemispheric winter, all models except GC tend to predict too little $SO_4^=$ in the source regions and too much in remote source regions (Fig. 11). Simultaneously, they over-predict SO_2 especially in remote regions (Fig. 12). There is good evidence that model HA simulates the northern hemispheric sulphur distribution best. In this case, results indicate that most models over-predict the dispersion of SO_x in the vertical particularly in the source regions (Fig. 5b: SO_x

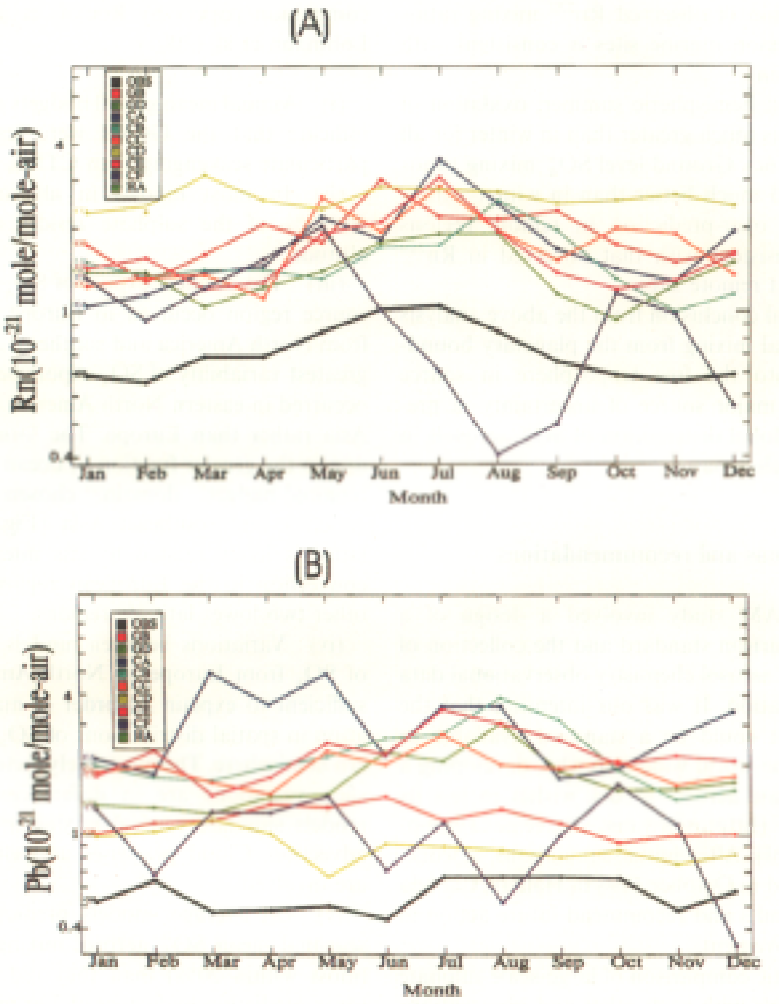

Fig. 16. Comparison of modeled and observed monthly mean mixing ratio of surface level ^{222}Rn and ^{210}Pb at Amsterdam Island (37.83°S, 72.53°E).

[0–1 km]/SO_x[total column]). Many models underestimate SO_2 oxidation in winter in source regions (Fig. 5c, mid-latitides) possibly due to too little cloud or a missing oxidation mechanism (e.g., Kasibhatla et al., 1997). Not oxidizing SO_2 which is less efficiently scavenged than $SO_4^=$ at this time of year, together with too vigorous vertical mixing into the free troposphere where horizontal wind speeds are higher leads to too much SO_x (mainly as SO_2) in the free troposphere as well as at the ground in remote regions. This is evident in over-prediction of SO_2 at ground level (Fig. 12) and the excessive amounts of SO_x in the northern hemisphere in winter of most models compared to HA (Fig. 7). Testing this with the amount of SO_x in the high latitude troposphere which generally reflects transport out of Europe and Russia into the Arctic (Fig. 7), shows that the exceptions are GB, GD and CF which perform closest to expectation along with HA. The fact that north of 45°N GC, CA and CC over-predict SO_x amounts in the vertical (Fig. 7) while simultaneously over-predicting the oxidation of SO_2 in the source region as well as remote region (Fig. 5c) suggests that the main explanation for excessive transport beyond the source region in these models is excessive mixing in the vertical and not lack of conversion of SO_2 to $SO_4^=$ in the source regions.

Over-prediction of observed Rn^{222} mixing ratios at remote region marine sites is consistent with this conclusion.

In northern hemispheric summer, oxidation of SO_2 to $SO_4^=$ is much greater than in winter for all models (Fig. 6c). Ground level $SO_4^=$ mixing ratios are simulated much better than in winter with a tendency to over-prediction in remote regions (Fig. 13) consistent with that observed in Rn^{222} predictions at remote sites.

The general conclusion from the above analysis is that vertical mixing from the planetary boundary layer into the free troposphere in source regions is a major source of uncertainty in predicting the global distribution of $SO_4^=$ aerosols in climate models today.

5. Conclusions and recommendations

The COSAM study involved a design of a model comparison standard and the collection of a new global aerosol chemistry observational data set for validation. It was our intention that the COSAM test could be a standard available to anyone on the world wide web who, developing a global sulphate aerosol model, wishes to test its performance (http://www.msc-smc.ec.gc.ca/armp/COSAM.html). After initial simulations, a workshop was held in October 1998 in Halifax, Canada to review results and recommend future action in model improvement.

A systematic comparison of large-scale sulphate aerosol models with each other and observations provided us with an estimate of the variance, between the population of sulphate aerosol models of the late 1990s and with insights into what causes that variance. This insight is valuable in assigning uncertainty to estimates of the impact of sulphate aerosols on climate that are undertaken by the Inter-governmental Panel on Climate Change (IPCC) as well as in improving models.

Participating in the COSAM study were 3 general circulation models (GCMs) that generate their own meteorological fields and 6 chemical transport models (CTMs) that are driven by gridded meterological fields produced from observations. Two of those CTMs (GD and CC) were essentially general circulation models nudged to analyzed winds. The following conclusions resulted from the analysis in this paper and 2 companion papers by Roelofs et al. (2001) and Lohmann et al. (2001).

(i) Annual mean global budgets of $^{222}Rn/^{210}Pb$ indicate that the GCMs were less efficient in particulate scavenging than CTMs.

(ii) In most models in all source regions, 40–60% of the sulphate resides above 2.5 km altitude.

(iii) The greatest export of SO_x from a major source region occurred in Europe and the least from North America and southeast Asia while the greatest variability of SO_x export between models occurred in eastern North America and southeast Asia rather than Europe. The former is in part due to the greater fraction of ocean surface in the regional-budget domain chosen for North America and southeast Asia (Fig. 1) while the latter is likely related to less intense simulated convection in the European region than in the other two lower latitude regions.

(iv) Variations between models in the export of SO_x from Europe or North America are not sufficient to explain an order of magnitude variation in spatial distributions of SO_x in the northern hemisphere. The most likely factors underlying such variations are in differences in how the models simulate vertical mixing and subsequent advection. Cloud processes as well as dynamics are involved.

(v) On average, models predict surface level seasonal mean $SO_4^=$ aerosol mixing ratios better (most within 20%) than they did those of SO_2 (over-prediction by factors of 2 or more). A higher resolution limited area model performed best by matching both parameters within 20%. In winter, there is a tendency to under-predict $SO_4^=$ close to source regions and over-predict in remote regions.

(vi) On the basis of global annual sulphur budgets as well as the spatial distributions of biogenic $SO_4^=$ and DMS, it was concluded that the two models with internally-generated-oxidant chemistry (a CTM and a GCM) oxidized DMS quite differently producing a mean annual tropospheric residence time of 2 versus 3.9 days. Thus in marine areas of high DMS emissions, OH concentrations predicted by the two models must differ considerably.

(vii) Vertical mixing of surface emissions from the planetary boundary layer into the free troposphere in source regions is a major source of

uncertainty in predicting the global distribution of SO_4^- aerosols in climate models today.

An outcome of the above analysis as well as the Halifax workshop is the realization that models are only as good as the data and process parameterizations that go into them. Model development is currently hindered by a lack of observations with which to test them. An integral part of this study has been the availability of standardized global anthropogenic inventories of sulphur species to the atmosphere and the assemblage of aerosol and related gaseous precursor observations by the World Aerosol Data Centre of the World Meteorological Organization's Global Atmosphere Watch (GAW) program. If aerosol models are to be improved in future, it is essential that globally coordinated research efforts continue to address emissions related to all atmospheric species that ultimately affect the distribution and optical properties of ambient aerosols. Furthermore, systematic atmospheric aerosol and related chemistry observations are required.

Currrent observational data have great shortcomings. First, there is a lack of a coherent global network of observations that will ultimately produce a world aerosol chemistry climatology. The networks, which currently exist, are principally located in industrially developed regions of Europe and North America. However, even in these areas the data produced from key sites are not always sufficient to address important scientific questions. For instance, data from continental boundary or coastal sites are required to understand long range transport of anthropogenic aerosols. As part of the European EMEP network protocol total sulphate is reported rather than non-sea salt sulphate. Sea salt sulphate is a natural part of the sea salt aerosol, which may dominate at coastal locations. Total sulphate data alone at these locations are thus much less valuable than non-sea salt sulphate data in understanding long range transport of anthropogenic aerosols. It is also very evident from the results in this paper that to validate a sulphate aerosol model, simultaneous measurements at a global network of sites is needed for, not only the aerosol, but also its gaseous precursors, in this case SO_2, DMS and key oxidants, H_2O_2 and O_3.

Second, there are major areas of the globe for which no data are available. In particular, there is sparse coverage in Asia, the southern hemisphere, equatorial and Pacific regions. This situation drastically worsened in 1996 when 15 southern hemisphere and Pacific sites were closed. There is now almost a total lack of measurements in these important regions, apart from some individual research sites such as those operated on Antarctica and Cape Grim. Thirdly, there are very few high altitude measurement sites. Only four sites provided data for the COSAM project and none were in the southern hemisphere. Finally, there is a dearth of vertical profile observations of major aerosol constituents and their gaseous precursors. A global research effort of aerosol related atmospheric chemistry measurements is urgently needed. Comprehensive long term systematic vertical profile studies at a few selected sites would be a great step forward.

If the ^{222}Rn and ^{210}Pb natural tracer pair are to be valuable model development tools more research is needed to improve knowledge of their emissions from continental areas in space and time and to systematically measure both species at aerosol network sites.

6. Acknowledgements

This work was supported by the World Meteorological Organization's working group on numerical experimentation (WGNE), the Climate Institute of Canada, the Meterological Service of Canada and the International Global Atmospheric Chemistry (IGAC) Project. Data for the IMPROVE and CAPMON networks were obtained via the Canadian, National Atmospheric Chemistry Database (NAtChem) group of Environment Canada in Toronto.

REFERENCES

Barrie, L. A., Olson, M. P. and Oikawa, K. K. 1989. The flux of anthropogenic sulphur into the Arctic from mid-latitudes. *Atmos. Envir.* **23**, 2502–2512.

Benkowitz, C. M., Scholtz, T., Pacyna, J., Tarrasón, L., Dignon, J., Voldner, E., Spiro, P. A. and Graedel, T. E. 1996. Global gridded inventories of anthropogenic emissions of sulphur and nitrogen. *J. Geophys. Res.* **101**, 29,239–29,253.

Chin, M., Rood, T. B., Lin, S.-J., Müller, J.-F. and Thompson, A. M. 2000. Atmospheric sulphur cycle simulated in the global model GOCART: model description and global properties. *J. Geophys. Res.* **105D**, 24,671–24,687.

Christensen, J. 1997. The Danish Eulerian hemispheric model – three dimensional air pollution model used for the arctic. *Atmos. Envir.* **31**, 4169–4191.

Dabdub, D. and Seinfeld, J. H. 1994. Numerical advective schemes used in air quality models – sequential and parallel implementation. *Atmos. Envir.* **28**, 3369–3385.

Dentener, F., Feichter, J. and Jeuken, A. 1999. Simulation of the transport of ^{222}Rn using on-line and off-line models at different horizontal resolutions: a detailed comparison with observations. *Tellus* **51B**, 573–602.

Erickson III, D. J., Ghan, S. J. and Penner, J. E. 1990. Global ocean-to-atmosphere dimethyl sulfide flux. *J. Geophys. Res.* **95**, 7543–7552.

Feichter, J. and Lohmann, U. 1999. Can relaxation technique be used to validate clouds and sulphur species in a GCM? *Q. J. Roy. Meteorol. Soc.* **125**, 1277–1294.

Giannakopoulos, C. 1998. *Modelling the impact of physical and removal processes on tropospheric chemistry*. PhD Thesis, University of Cambridge, Cambridge, England.

Ghan, S., Laulainen, N., Easter, R., Wagener, R., Nemesure, S., Chapman, E., Zhang, Y. and Leung, R. 2001. Evaluation of aerosol direct radiative forcing in MIRAGE. *J. Geophys. Res.* **D106**, 5295–5316.

Graf, H., Feichter, J. and Langmann, B. 1997. Volcanic sulfur emissions: Estimates of source strength and its contribution to the global sulfate distribution. *J. Geophys. Res.* **102**, 10,727–10,738.

Houweling, S., Dentener, F. and Lelieveld, J. 1998. The impact of nonmethane hydrocarbon compounds on tropospheric photochemistry. *J. Geophys. Res.* **103**, 10,673–10,696.

Jacob, D. J. Prather, M. J., Rasch, P. J., Shia, R.-L. et al. 1997. Evaluation and intercomparison of global transport models using ^{222}Rn and other short lived tracers. *J. Geophys. Res.* **102D**, 5953–5970.

Kasibhatla, P., Chameides, W. L. and St. John, J. 1997. A three dimensional global model investigation of seasonal variations in the atmospheric burden of atmospheric sulfate aerosols. *J. Geophys. Res.* **102**, 3737–3760.

Kettle, A.J. et al. 1999. A global database of sea surface dimethylsulfide (DMS) measurements and a procedure to predict sea surface DMS as a function of latitude, longitude, and month. *Global Biogeochem. Cycles* **13**, 394–444.

Koch, D. M., Jacob, D. J., Rind, D., Chin, M. and Tegen, I. 1999. Tropospheric sulphur simulation and sulfate direct radiative forcing in the Goddard Institute for Space Studies general circulation model. *J. Geophys. Res.* **104**, 23,799–23,822.

Kritz, M. A., Leroulley, J.-C. and Danielsen, E. F. 1990. The China Clipper — fast advective transport of radon-rich air from the Asian boundary layer to the upper troposphere near California. *Tellus* **42B**, 46–61.

Kritz, M. A., Rosner, S. W. and Stockwell, D. Z. 1998. Validation of an off-line three-dimensional chemical transport model using observed radon profiles: Part 1. Observations. *J. Geophys. Res.* **103D**, 8425–8432.

Law, K. S., Plantevin, P.-H., Shallcross, D. E., Rogers, H., Grouhel, C., Thouret, V., Marenco, A. and Pyle, J. A. 1998. Evaluation of modelled O_3 using MOZAIC data. *J. Geophys. Res.* **103**, 25,721–25,740.

Liss, P. S. and Merlivat, L. 1986. Air–sea exchange rates: introduction and synthesis. In: *The rôle of air–sea exchange in geochemical cycling*, ed. P. Buat-Menard, pp. 113–127. D. Reidel Publishing Company, Berlin, Germany.

Lohmann, U., Von Salzen, K., McFarlane, N., Leighton, H. G. and Feichter, J. 1999. The tropospheric sulfur cycle in the Canadian general circulation model. *J. Geophys. Res.* **104**, 26,833–26,858.

Lohmann U., Leaitch, R., Law, K., Barrie, L., Yi, Y., Bergman, D., Chin, M., Easter, R., Feichter, J., Jeuken, A., Kjellström, E., Koch, D., Land, C., Rasch, P. and Roelofs, G.-J. 2001. Comparison of the vertical distributions of sulfur species from models participated in the COSAM exercise with observations. *Tellus* **53B**, this issue.

Penner, J. E., Bergmann, D., Walton, J. J., Kinnison, D., Prather, M. J., Rotman, D., Price, C., Pickering, K. E. and Baugheum, S. L. 1998. An evaluation of upper troposphere NO_x with two models. *J. Geophys. Res.* **103**, 22,097–22,113.

Preiss, N., Melieres, M. A. and Pourchet, M. 1996. A compilation of data on lead 210 concentration in surface air and fluxes at the air surface interface and water sediment interfaces. *J. Geophys. Res.* **101D**, 28,847–28,862.

Pyle, J. and Prather, M. 1996. Global tracer transport models. In: *Report of a scientific symposium*, V.24, WMO TD, Geneva, Switzerland.

Rasch, P. J., Barth, M. C., Kiehl, J. T., Schwartz, S. E. and Benkovitz, C. M. 2000a. A description of the global sulphur cycle and its controlling processes in the National Center for Atmospheric Research Community Climate Model, Version 3. *J. Geophys. Res.* **105**, 1367–1385.

Rasch, P.J., Feichter, J., Law, K., Mahowald, N.,

Penner, J. et al. 2000b. An assessment of scavenging and deposition processes in global models: results from the WCRP Cambridge workshop of 1995. *Tellus* **52B**, 1025–1056.

Roelofs, G. J., Lelieveld, J. and Ganzeveld, L. 1998. Simulation of global sulphate distribution and the influence on effective cloud drop radii with a coupled photochemistry-sulfur cycle model. *Tellus* **50B**, 224–242.

Roelofs, G. J., Kasibhatla, P., Barrie, L., Bergmann, D., Bridgeman, C., Chin, M., Christensen, J., Easter, R., Feichter, J., Jeuken, A., Kjellström, E., Koch, D., Land, C., Lohmann, U. and Rasch, P. 2001. Analysis of regional budgets of sulfur species modelled for the COSAM exercise. *Tellus* **53B**, this issue.

Sirois, A. and Barrie, L. A. 1999. Arctic lower tropospheric aerosol trends and composition at Alert, Canada: 1980–1995. *J. Geophys. Res.* **104D**, 11,599–11,618.

Spiro, P. A., Jacob, D. J. and Logan, J. A. 1992. Global inventory of sulfur emissions with 1° × 1° resolution. *J. Geophys. Res.* **97**, 6023–6036.

Staubes, R. and Georgii, H. W. 1993. Measurements of atmospheric and sea water DMS concentrations in the Atlantic, the Arctic and Antarctic region. In: *Dimethylsulphide, oceans atmosphere and climate*, eds. G. Restelli and G. Angeletti. Kluwer 95–102, Academic Publishers, 399 pp.

Trenberth, K. E., Olson, J. G. and Large, W. G. 1989. *A global ocean wind stress climatology based on ECMWF analysis*. NCAR/TN-338 + STR. NCAR Technical note. August. NCAR, Boulder, CO, USA.